

**Anoxia reduces whole cell permeability in cortical neurons of the anoxia tolerant turtle,  
*Chrysemys picta belli***

by

**Himesh S. Ghai**

A thesis submitted in conformity with the requirements  
for the degree of Masters of Science  
Graduate Department of the Department of Zoology  
University of Toronto



National Library  
of Canada

Acquisitions and  
Bibliographic Services

395 Wellington Street  
Ottawa ON K1A 0N4  
Canada

Bibliothèque nationale  
du Canada

Acquisitions et  
services bibliographiques

395, rue Wellington  
Ottawa ON K1A 0N4  
Canada

*Your file* *Votre référence*

*Our file* *Notre référence*

The author has granted a non-exclusive licence allowing the National Library of Canada to reproduce, loan, distribute or sell copies of this thesis in microform, paper or electronic formats.

The author retains ownership of the copyright in this thesis. Neither the thesis nor substantial extracts from it may be printed or otherwise reproduced without the author's permission.

L'auteur a accordé une licence non exclusive permettant à la Bibliothèque nationale du Canada de reproduire, prêter, distribuer ou vendre des copies de cette thèse sous la forme de microfiche/film, de reproduction sur papier ou sur format électronique.

L'auteur conserve la propriété du droit d'auteur qui protège cette thèse. Ni la thèse ni des extraits substantiels de celle-ci ne doivent être imprimés ou autrement reproduits sans son autorisation.

0-612-46188-2

Canada

**ABSTRACT**

Whole cell permeability is reduced in the brain of the anoxia tolerant turtle,  
*Chrysemys picta belli*

Himesh S. Ghai

Master of Science, 1999

Department of Zoology, University of Toronto

The western painted turtle, *Chrysemys picta belli*, is one of the most anoxia tolerant species presently known. It has been postulated that anoxia tolerant species can acutely reduce membrane ion permeability (Channel Arrest) as a means of reducing energy requirements during anoxia. To test this, whole cell conductance ( $G_w$ ) was measured in turtle neurons using a whole cell patch clamp technique. Perfusion of cortical sheets with control (normoxic) saline did not result in any significant changes in  $G_w$ . However, anoxic and adenosine (200 $\mu$ M) perfusions significantly reduced  $G_w$ , an effect which was inhibited with the inclusion of EGTA (5mM) in the recording electrode. Additionally, perfusion of cortical sheets with high levels of extracellular calcium (4,8mM) also reduced  $G_w$ . To determine if the observed changes in  $G_w$  can be attributed to changes in gap junction permeability, a whole cell patch clamp technique was employed to measure changes in whole cell capacitance ( $C_w$ ) during normoxic, anoxic, high adenosine (200 $\mu$ M) and high calcium (4mM) perfusions. Whole cell capacitance values calculated under these conditions did not change significantly when compared to control values. Additionally, injection of lucifer yellow into turtle brain neurons did not show dye propagation to neighbouring cells during either normoxic or anoxic perfusion. These data suggest that whole-cell conductance does decrease with the transition to anoxia in turtle brain and that the response is not entirely intrinsic to the tissue but may be systemic. Furthermore, the lack of dye propagation during conditions that decrease  $G_w$  suggests that gap junctions are not involved in the observed anoxia-mediated changes in  $G_w$ .

## **ACKNOWLEDGEMENTS**

Les Buck, for giving me the opportunity to discover my true potential, for always being supportive and creating an atmosphere in the lab that breeds productivity and self-confidence. Thanks for all your invaluable knowledge and guidance in all things vertebrate!

Janani Balasubramaniam (Lisa) and Damian Shin (Martin) for making my tenure in the lab an extremely enjoyable experience. Thanks for not telling Les about the other things that I broke and/or lost!

Stephen Tobe and John F. McDonald, for their helpful suggestions. Zhigang Xiong, for helping me understand the capacitance work.

To my family, for their love and unwavering support, without which I would still be “lost in space”. A special thanks to my brother Jitesh for being my greatest critic and supporter, all in one.

To Kiran, who has been extremely patient with my unpredictable mood swings and frustrations, forever convinced of my strengths and always willing to help me overcome my weaknesses.

To my friends, who just don't understand that its tough to get a turtle to stick its head out! You do what you must to get the job done, dirty fingers and all!

**“Satnam Srivaheguru”**

## ORGANIZATION OF THE THESIS

Part of this thesis has been published in *American Journal of Physiology* (Ghai, H. S. and Buck, L. T. (1999) Acute reduction in Whole cell conductance in anoxic turtle brain.. *Am. J. Physiol.* 277: R887-R893.) All experiments were performed by myself and Dr. L. T. Buck provided invaluable aid in the form of discussions, editorial comments on the manuscript and financial support for all aspects of this thesis.

## TABLE OF CONTENTS

<b>CONTENT</b>	<b>PAGE</b>
Abstract	i
Acknowledgements	ii
Organisation of thesis	iii
Table of contents	iv
List of figures and tables	vi
<b>INTRODUCTION</b>	<b>1</b>
The Mammalian Brain: A model of anoxia sensitivity	3
K <sup>+</sup> efflux	4
Na <sup>+</sup> influx and cellular depolarisation	10
Ca <sup>2+</sup> influx and cellular excitotoxicity	11
The Turtle Brain: A model of anoxia tolerance	19
Reduced glycolytic activity and “Metabolic Arrest”	21
“Channel Arrest” and “Spike Arrest” contribute to metabolic depression in the anoxic turtle brain	28
K <sup>+</sup> channels	29
Na <sup>+</sup> channels	32
Ca <sup>2+</sup> channels	33
Adenosine	33
<b>RESEARCH PROPOSAL</b>	<b>38</b>
Hypothesis 1: Does whole cell permeability change in the anoxic Turtle brain?	38
Hypothesis 2: Are gap junctions involved in modulating whole cell Permeability in the anoxic turtle brain?	39
<b>MATERIALS AND METHODS</b>	<b>41</b>
Animals	41
Dissection and experimental configuration	41
Whole cell conductance and capacitance measurements	42
Whole cell conductance experiments	50
Whole cell capacitance experiments	53
Statistical Analysis	54

<b>RESULTS</b>	<b>55</b>
Whole cell conductance experiments	55
Whole cell capacitance experiments	74
<b>DISCUSSION</b>	<b>81</b>
<b>SUMMARY AND CONCLUSION</b>	<b>90</b>
<b>REFERENCES</b>	<b>92</b>

<b>LIST OF FIGURES AND TABLES</b>		<b>PAGE</b>
Figure 1.	Changes in metabolite and extracellular ion concentrations in ischemic rat brain	5-6
Figure 2.	Reversible blockade of hypoxia induced inward current by barium	8-9
Figure 3.	Effect of Tetrodotoxin on ischemia-induced $K^+$ flux	12-13
Figure 4.	Postulated mechanisms of $Ca^{2+}$ mediated anoxic ischemic injury	18-19
Figure 5.	Changes in anoxic turtle brain ATP, ADP and AMP levels	22-23
Figure 6.	Heat dissipation during anoxia in turtle cortical slices	25-26
Figure 7.	Changes in extracellular $K^+$ in normoxic/anoxic turtle brain	30-31
Figure 8.	Adenosine and anoxia induced changes in turtle brain blood flow	35-36
Figure 9A.	Typical whole cell current response	44-45
Figure 9B.	Current/Voltage relationship	46-47
Figure 10.	Typical whole cell capacitance response	48-49
Figure 11.	Effect of normoxic and anoxic perfusions on $G_w$ (+EGTA)	56-57
Figure 12.	Effect of mimic aCSF perfusion on $G_w$	58-59
Figure 13.	Changes in $G_w$ during control and anoxic tissue perfusions (-EGTA)	60-61
Figure 14.	Effect of low pH and high $Mg^{2+}$ tissue perfusions on $G_w$	62-63
Figure 15.	Changes in $G_w$ during 4 and 8mM $Ca^{2+}$ tissue perfusions	65-66
Table 1.	Tissue energy charge and [ATP] under high $Ca^{2+}$ incubation	67
Figure 16.	Effect of adenosine treatment on $G_w$ (+/- EGTA)	68-69
Figure 17.	$G_w$ values obtained during acute tissue perfusion with CPA solutions	70-71
Figure 18.	Effect of DPCPX on $G_w$ during adenosine and anoxic perfusions	72-73
Figure 19.	Effect of normoxic and anoxic perfusions on $C_w$	75-76
Figure 20.	$C_w$ values obtained during calcium and adenosine perfusions	77-78



Figure 21.	<b>Lucifer yellow loaded neurons under normoxic and anoxic tissue Perfusions</b>	79-80
Figure 22.	<b>Postulated mechanisms and possible sites of ion channel regulation</b>	86-87

## INTRODUCTION

The vertebrate brain requires a continuous supply of energy in the form of ATP in order to function. Theoretically, under aerobic conditions, 6 moles of oxygen are consumed to oxidize 1 mole of glucose to carbon dioxide (CO<sub>2</sub>) and water (H<sub>2</sub>O), producing 34 moles of ATP via mitochondrial oxidative phosphorylation and 2 moles from glycolysis. These processes result in a total of 36 moles of ATP produced per mole of glucose (Hochachka and Somero, 1984). Alternatively, anaerobic glycolysis, a less efficient system of ATP production, yields only 2 moles of ATP with the breakdown of 1 mole of glucose to 2 moles of lactate. As such, more than 95% of vertebrate brain ATP is produced using aerobic pathways of metabolism. Much of this ATP is used to support brain electrical activity, a prerequisite for inter-neuronal communication and integrated whole brain function. It is estimated that 50-60% of the total neuronal energy budget is used to maintain ionic gradients across the cell membrane. This is predominantly via Na<sup>+</sup>/K<sup>+</sup> ATPase which continually utilises ATP to re-establish transcellular ionic gradients after neuronal electrical and synaptic activity (Hansen, 1985; Lutz, 1992). Under normoxic conditions, the brain is able to function normally, producing enough ATP to match ATP consumption so that brain [ATP] (ATP concentration) and the rate of ATP turnover remains unchanged over a wide range of energy consuming activities.

The brain of most vertebrates, however, is extremely sensitive to energy failure. During oxygen limiting conditions such as ischemia, hypoxia and most notably, anoxia (the absence of oxygen), the vertebrate brain has almost no ability to continue normal neuronal function. One reason for the vertebrate brain's extreme sensitivity to energy failure is its poor ability to store glucose and oxygen. Typically, the glycogen content of the mammalian

brain is approximately 2-4 $\mu\text{mol/g}$  (Siesjo, 1978) and compared to other organs, the brain has a low blood volume (1% of wet weight) holding about 0.09 $\mu\text{mol O}_2/\text{g}$  brain tissue (Lutz and Nilsson, 1997). During anoxia, brain glycogen stores would be depleted within minutes if the brain continues to function under aerobic rates of glucose consumption (0.8 $\mu\text{mol/g}\cdot\text{min}$ ) (Siesjo, 1978). Furthermore, in the ischemic brain, normal rates of oxygen consumption (1.6-5 $\mu\text{mol/g}\cdot\text{min}$ ) will deplete the brain's already limited supply of oxygenated blood within a few seconds (Siesjo, 1978). In the face of oxygen deprivation, the principle supply of ATP for the energetically demanding maintenance of neuronal function will come from anaerobic glycolysis, which will provide less than 5% of the ATP available to the brain under normal (fully aerobic) conditions (Lutz et. al., 1985). The drastic reduction in ATP production in the absence of a comparable reduction in ATP demand will result in the rapid depletion of brain ATP stores, creating an energy imbalance, which disrupts neuronal ionic homeostasis within a matter of minutes (Doll, 1993a). In fact, a major cause of brain death is the disruption of cellular ionic gradients due to the inability of the  $\text{Na}^+/\text{K}^+$  ATPase to function in the face of depleting brain ATP levels. This is considered to be a key precursor to irreversible neuronal structural damage (Hansen, 1985). Although the general pattern of degenerative changes in cellular ionic gradients is probably common to all vertebrates with changes only in the time scale due to differences in body temperature and metabolism (Lutz and Nilsson, 1997), the mammalian brain is especially anoxia-sensitive owing to its high obligatory rate of ATP consumption and inability to maintain neuronal ionic homeostasis during anoxia.

## THE MAMMALIAN BRAIN: A MODEL OF ANOXIA SENSITIVITY

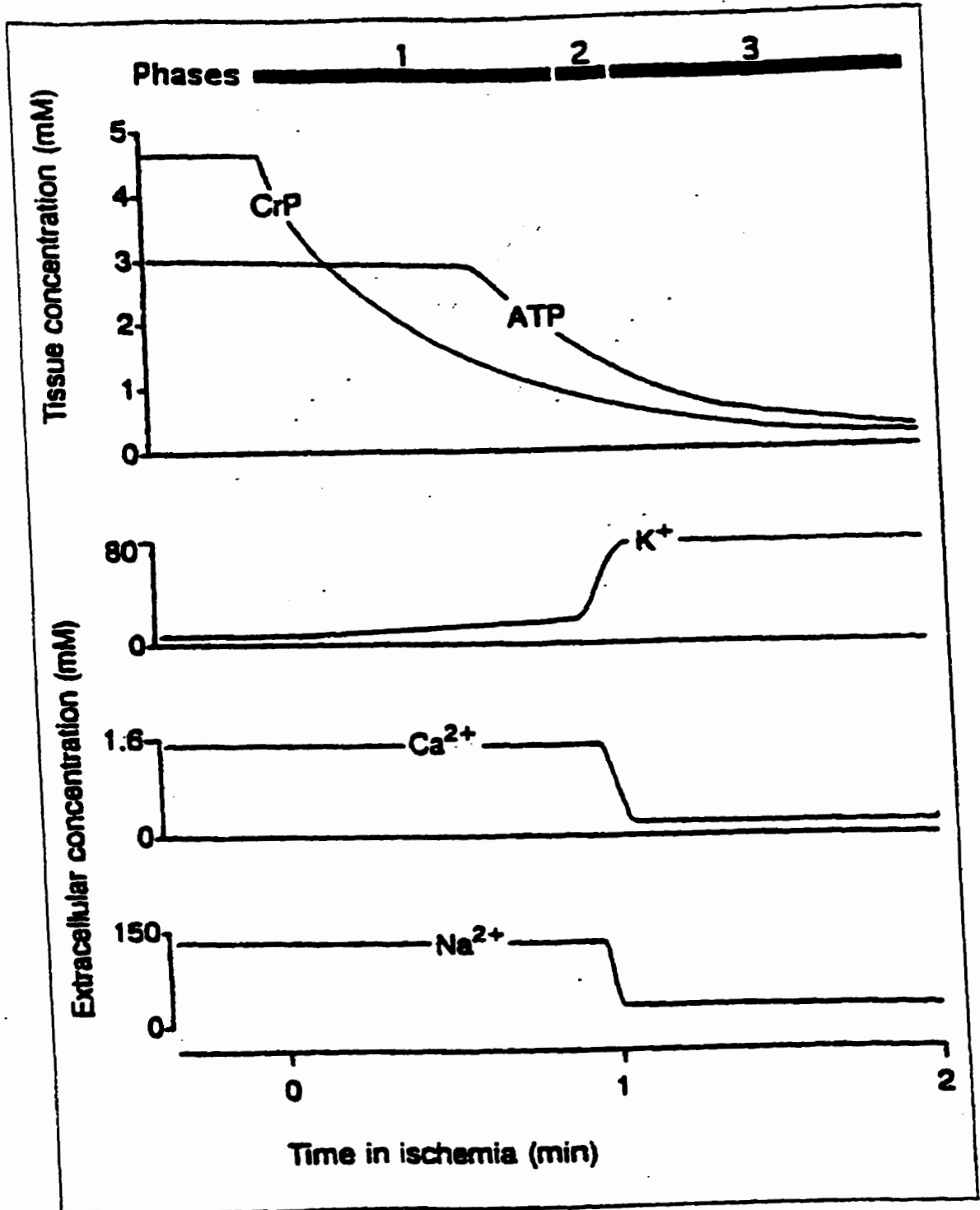
The mammalian brain is an example of an anoxia-sensitive vertebrate brain. In the mammalian brain, inhibition of oxygen delivery compromises ATP production via aerobic metabolic pathways, resulting in a 75% reduction in ATP within the first minute of exposure (Ridge, 1972). Initially, a rapid decline in creatine phosphate (CrP) and ATP levels is detected, lasting approximately 1-2 minutes (Fig. 1) and results in a “Pasteur effect”. The depletion of the available ATP quickly disrupts energy dependent  $\text{Na}^+/\text{K}^+$  exchange across the neuronal membrane and there is a net movement of ions across the cell membrane down their concentration gradients. Consequently, there is an increase in extracellular  $\text{K}^+$  ( $[\text{K}^+]_o$ ) through ATP-dependent  $\text{K}^+$  channels (see below), resulting in what is termed “anoxic depolarization” (AD) and an increase in cytosolic  $\text{Ca}^{2+}$  via mechanisms that are presently unclear.

At the presynaptic terminal, these events result in the release of excitatory amino acids (EAAs), glutamate and aspartate, which are thought to be a cause of anoxic/ischemic brain damage. There is evidence that at the post-synaptic membrane, glutamate activates the Kainate (K) and Quisqualate (Q) receptors and increases their permeabilities to monovalent cations, allowing sodium into the cell and  $\text{K}^+$  out of the cell, resulting in cellular depolarization. The depolarization also facilitates the glutamate mediated activation of the N-methyl-D-aspartate receptor, resulting in a massive flux of  $\text{Ca}^{2+}$  into the cell. This increased permeability of the post-synaptic neuron to cations, particularly  $\text{Ca}^{2+}$ , initiates a cascade of intracellular and extracellular excitotoxic events, ultimately causing cell death (Choi, 1992).

A great deal of interest has developed in understanding the cellular mechanisms involved in mediating the responses of both tolerant and intolerant models to energy/oxygen limiting situations. More specifically, the movement of ions such as  $\text{Ca}^{2+}$ ,  $\text{Na}^+$ , and  $\text{K}^+$  across the cell membrane via voltage-gated and/or receptor-gated channels has been studied in order to provide further understanding of the role of these ions in both normal and energy limited conditions. Initially, I will review the literature relevant to  $\text{K}^+$ ,  $\text{Na}^+$ , and  $\text{Ca}^{2+}$  movement through voltage dependent and receptor-gated ion channels during ischemia, anoxia or hypoxia in the mammalian brain. The remainder will focus on understanding the mechanisms of anoxia tolerance and how these injurious ion fluxes are prevented in the anoxia tolerant turtle brain.

***K<sup>+</sup> Efflux:*** In the anoxic mammalian cerebral cortex,  $\text{K}^+$  efflux occurs in two distinct phases. In phase 1,  $[\text{K}^+]_o$  increases gradually from 3-15mM (60-100s) with no major changes in extracellular  $\text{Na}^+$ ,  $\text{Ca}^{2+}$ ,  $\text{Cl}^-$  (Fig. 1). A decrease in brain electrical activity (Lipton and Whittingham, 1982) is also observed at this time, most likely due to hyperpolarization of the neurons. Several studies have also shown that anoxia in hippocampal neurons produces an early hyperpolarization which is due to the activation of  $\text{K}^+$  channels and a rapid blockade of synaptic transmission (Fujiwara et. al., 1987; Krnjevic and Leblond, 1988). Folbergrova et. al. (1990) examined whether the initial release of  $\text{K}^+$  during anoxia can be related to a rise in intracellular  $\text{Ca}^{2+}$ .

**Fig. 1.** Changes in ATP, creatine phosphate (CrP) and extracellular ion concentrations during ischemia in the rat brain. Reciprocal changes in ion concentrations occur simultaneously in the cytosolic compartment of the cell as a result of ion movement across the cell membrane. The changes in ion distribution occur in three distinct phases. Phase 1 is characterized by a steady efflux of  $K^+$ . Phase 2 begins approximately 1 minute after Phase 1 induction during which rapid fluxes in  $K^+$ ,  $Ca^{2+}$  and  $Na^+$  are seen. Phase 3 is characterized by a resultant steady state in ion levels following phase 2. Reprinted from Lutz and Nilsson, (1997).

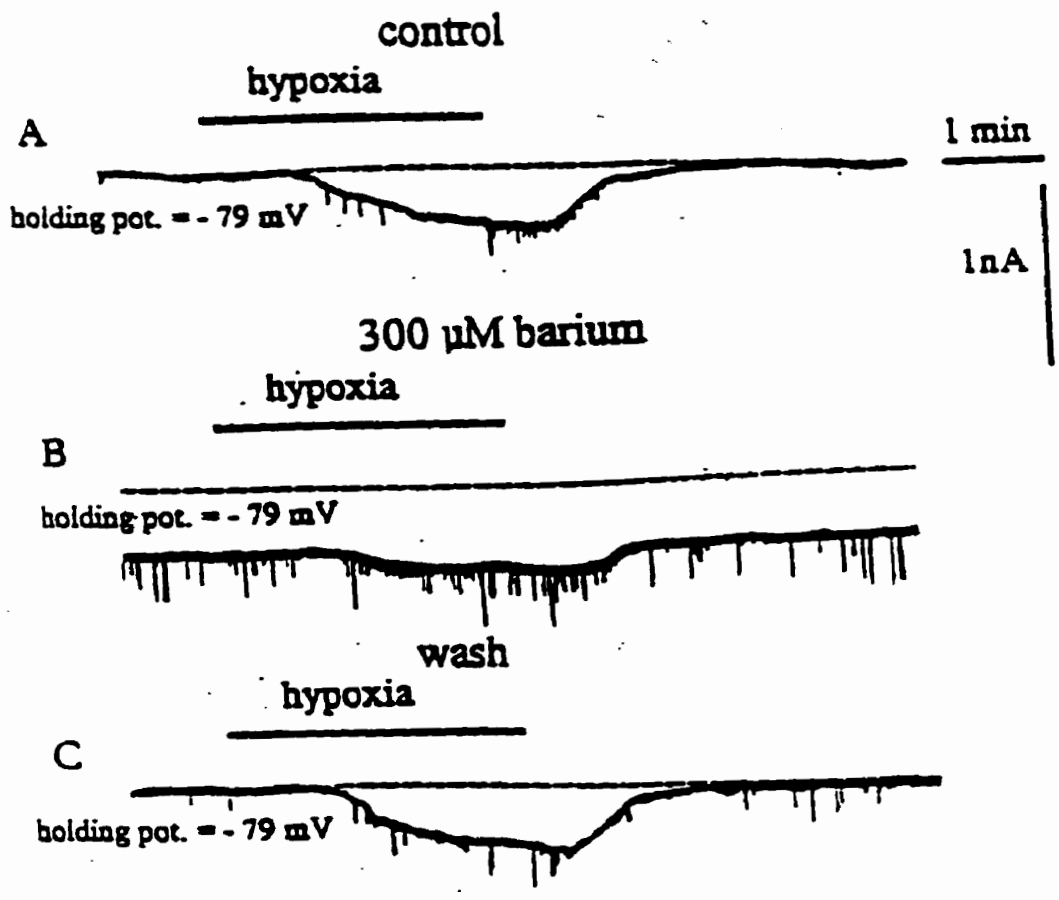


The authors found that  $[K^+]_o$  rose before ATP levels had decreased appreciably. Furthermore, the activity of *phosphorylase a* (an estimate of intracellular  $Ca^{2+}$  activity) also increased suggesting that a rise in  $[Ca^{2+}]_i$  may trigger a  $K^+$  conductance. It was not demonstrated as to how an increase in  $[Ca^{2+}]_i$  occurs since the results were not correlated to ionic fluxes, although the initial rise in intracellular  $Ca^{2+}$  may be due to release from internal stores such as the sarcoplasmic reticulum.

In vitro studies on cultured neurons suggest that the ATP sensitive  $K^+$  channel ( $K_{ATP}$ ) is intimately involved in mediating the  $K^+$  efflux under ischemic conditions (Ben-Ari, 1990). The  $K_{ATP}$  channel is a unique ionophore in that it appears to reflect cell metabolism. In the substantia nigra, treatment with  $CN^-$  resulted in an increase in outward  $K^+$  currents, resulting in a hyperpolarizing effect. This response was abolished upon application of sulphonylurea tolbutamide, a potent blocker of the  $K_{ATP}$  channel (McGroarty and Greenfield, 1996). The results suggest that in the substantia nigra, the  $K_{ATP}$  channel plays a key role in normal mechanisms of neuronal homeostasis in response to anoxia and ischemia. Calabresi et. al. (1995) have shown that hypoxia induced electrical responses are significantly reduced by pre-treating the slices with Barium, a  $K^+$  channel blocker (Fig. 2). Mourre et. al. (1989) have reported that glibenclamide, a potent sulphonylurea ligand that targets  $K_{ATP}$  channels, blocks the early hyperpolarization and a considerable increase of the post synaptic hyperpolarization produced by anoxia in hippocampal slices, suggesting that the  $K_{ATP}$  channels may play a role in the electrical events leading to blockade of synaptic transmission during anoxia. It could be possible that the first phase of  $K^+$  efflux from neuronal cells might be due to opening of



**Fig. 2.** Barium, a  $K^+$  channel blocker, reversibly reduces the inward current induced by hypoxia. **(A)** Under control conditions, hypoxia generates an inward current in the cortical slice. **(B)** Incubation of the slice in  $300\mu\text{M}$  barium reduces the amplitude of the hypoxia-induced inward current. **(C)** After the wash-out of the effect of barium the inward current is recovered. Reprinted from Calabresi et. al. (1995).



the  $K_{ATP}$  channels. Additionally, blockade of the  $K_{ATP}$  channels reduced the ischemia-induced rise in  $[K^+]_o$  indicating the involvement of the  $K_{ATP}$  channels in ischemia induced  $K^+$  efflux (Xie and Ziskind-Conhaim, 1995). In contrast to this, Krnjevic and Leblond (1988) found that in the CA1 region the other sulfonylurea ligand-tolbutamide, does not reduce the anoxic hyperpolarization. This discrepancy may be due to regional differences in the distribution of  $K_{ATP}$  channels. Regional variability has been demonstrated in the sensitivity to hypoxia by Donnelly et. al. (1992), who found that brain stem neurons depolarize at a faster rate than cortical neurons. Another important aspect to consider is that there could be other types of  $K^+$  channels involved in mediating the  $K^+$  flux in the anoxic mammalian brain.

In phase 2, once  $[K^+]_o$  reaches 13-15mM, there is a sudden efflux of  $K^+$  from cells and uptake of  $Ca^{2+}$  and  $Na^+$  (Fig. 1). It seems possible that  $K^+$  efflux in the initial stage could set the stage for the  $K^+$  efflux in the second stage, possibly via the action of various types of voltage-gated  $K^+$  channels (Haddad and Jiang, 1993). Furthermore, Yu et. al. (1999) have demonstrated that  $K^+$  efflux through NMDA receptor activation results in cellular apoptosis. This suggests that the observed anoxia induced increase in  $[K^+]_o$  may be mediated by channel types other than voltage-gated  $K^+$  channels. However, the mechanistic nature of the rapid increase in the permeability of  $K^+$  ions is not well understood.

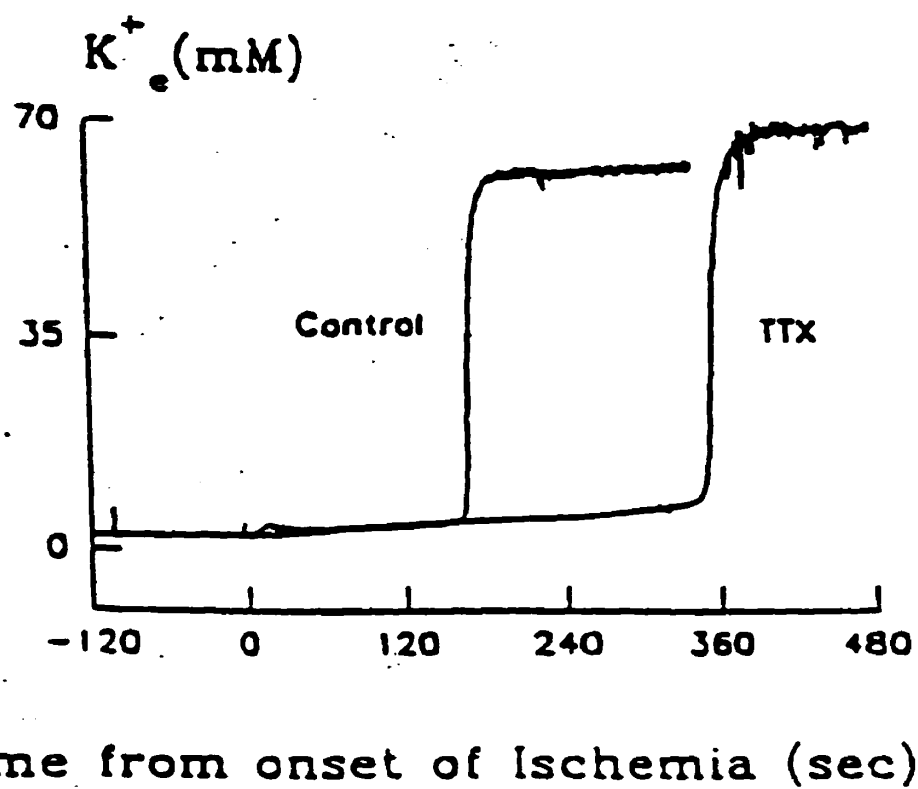
***Na<sup>+</sup> influx and cellular depolarization:*** Neuronal  $Na^+$  influx has been suggested to contribute to the “anoxic depolarization” (AD) in mammalian brain (Ashton et. al., 1990). Voltage sensitive  $Na^+$  channels have several receptor sites sensitive to neurotoxins such as tetrodotoxin (TTX) and veratridine. These neurotoxins bind with the protein components of the  $Na^+$  channel either to inhibit  $Na^+$  flux through the channel or to facilitate  $Na^+$  movement through the channel. Gleitz et. al. (1996) have shown that  $Na^+$  influx induced by veratridine,

a voltage dependent  $\text{Na}^+$  channel agonist, results in the inhibition of anaerobic glycolysis (inhibition of lactate production), which could further deplete ATP levels resulting in loss of ionic gradients and cell death. Furthermore, Xie et. al. (1994) have shown that TTX perfusion of rat brain postponed the occurrence of ischemia-induced AD by 65%, as indicated by a significantly reduced  $\text{K}^+$  efflux in TTX treated brains compared to control (Fig. 3). These results suggest that  $\text{Na}^+$  influx via voltage gated  $\text{Na}^+$  channels is a major factor leading to cell depolarization. Since  $\text{Na}^+$  mediated depolarization potentially activates voltage gated  $\text{Ca}^{2+}$  and  $\text{K}^+$  channels, the anoxic injury observed in CA1 neurons could be mediated by  $\text{Na}^+$  (Friedman and Haddad, 1994). Thus,  $\text{Na}^+$  might be involved in the morphological and electrical changes that occur in the mammalian brain during anoxic/ischemic exposure.

***Ca<sup>2+</sup> influx and cellular excitotoxicity:*** Among the various events involved in the mammalian brain's response to anoxia, increased  $\text{Ca}^{2+}$  influx across the cell membrane has received particular attention. This influx and subsequent rise in free cytosolic  $\text{Ca}^{2+}$  during anoxia/ischemia may result from (1) massive activation of voltage sensitive  $\text{Ca}^{2+}$  channels (VSCC) (2)  $\text{Ca}^{2+}$  influx via N-methyl-D-aspartate (NMDA) receptors and (3) modulation of alpha-amino-3-hydroxy-5-methyl-isoxazole-4-propionate (AMPA) and/or Kainate (KA) channels. These channel types can be manipulated directly by a vast array of organic and inorganic agents.

Selective blockade of *neuronal* N-type VSCCs has been demonstrated to be consistently neuroprotective in rodent models of both global and focal cerebral ischemia (Buchan et.al., 1994; Valentino et. al., 1993). This channel type has been found to be located on the presynaptic terminals of many neurons, especially in the CA3 region of the hippocampus (Westenbroek et. al., 1992). Indeed, Bowersox et.al. (1996) have shown that

**Fig. 3.** Effect of the Na<sup>+</sup> channel blocker Tetrodotoxin (TTX) on ischemia-induced K<sup>+</sup> flux and corresponding anoxic depolarization. The TTX treatment markedly delays the increase in extracellular K<sup>+</sup> and occurrence of anoxic depolarization compared to control conditions. Adapted from Xie et. al. (1994).



reducing  $\text{Ca}^{2+}$  influx via blockade of presynaptic N-type  $\text{Ca}^{2+}$  channels is effective in attenuating, if not preventing, neuronal degeneration in the neocortex of the rat. Electrophysiological studies and transmitter release studies have clearly shown a functional role for presynaptic N-type channels in glutamate and monoamine release (Wheeler et. al., 1994; Gaur et. al., 1994) suggesting that blockade of this channel type may be important in attenuating excitatory neurotransmitter release presynaptically .

Several studies have demonstrated that the blockade of the presynaptic *low conductance* L-type  $\text{Ca}^{2+}$  channels is also neuroprotective against glutamate induced toxicity in cerebellar granule cells (Simen and Miller, 1998; Pizzi et. al., 1991). Support for the involvement of L-type  $\text{Ca}^{2+}$  channels in mediating the neuronal response to energy limitation comes from Maruyama et. al. (1994), who have shown that application of Diltiazem (DILT), a L-type  $\text{Ca}^{2+}$  channel blocker to hippocampal synaptic membranes results in reduced  $\text{Ca}^{2+}$  influx and a greater measure of protection against neuronal hypoxia. These studies suggest that both the N and L-type  $\text{Ca}^{2+}$  channels may mediate the influx of  $\text{Ca}^{2+}$  resulting in a massive release of glutamate stored in synaptic vesicles of the presynaptic membrane. Although release of other excitatory NTs (aspartate, dopamine) occurs, glutamate release is thought to be a major cause of anoxic neuronal cell destruction.

At the post-synaptic terminal, glutamate binds to its receptors, triggering further influxes of  $\text{Ca}^{2+}$  and  $\text{Na}^+$ . This increased permeability of the post-synaptic neuron to cations, particularly  $\text{Ca}^{2+}$ , initiates a cascade of intracellular and extracellular excitotoxic events, ultimately causing cell death. A wealth of evidence strongly suggests that the three glutamate receptor subtypes; NMDA, AMPA, and KA mediate the excitotoxic events associated with combined oxygen and glucose, or oxygen deprivation. Specific agonists of

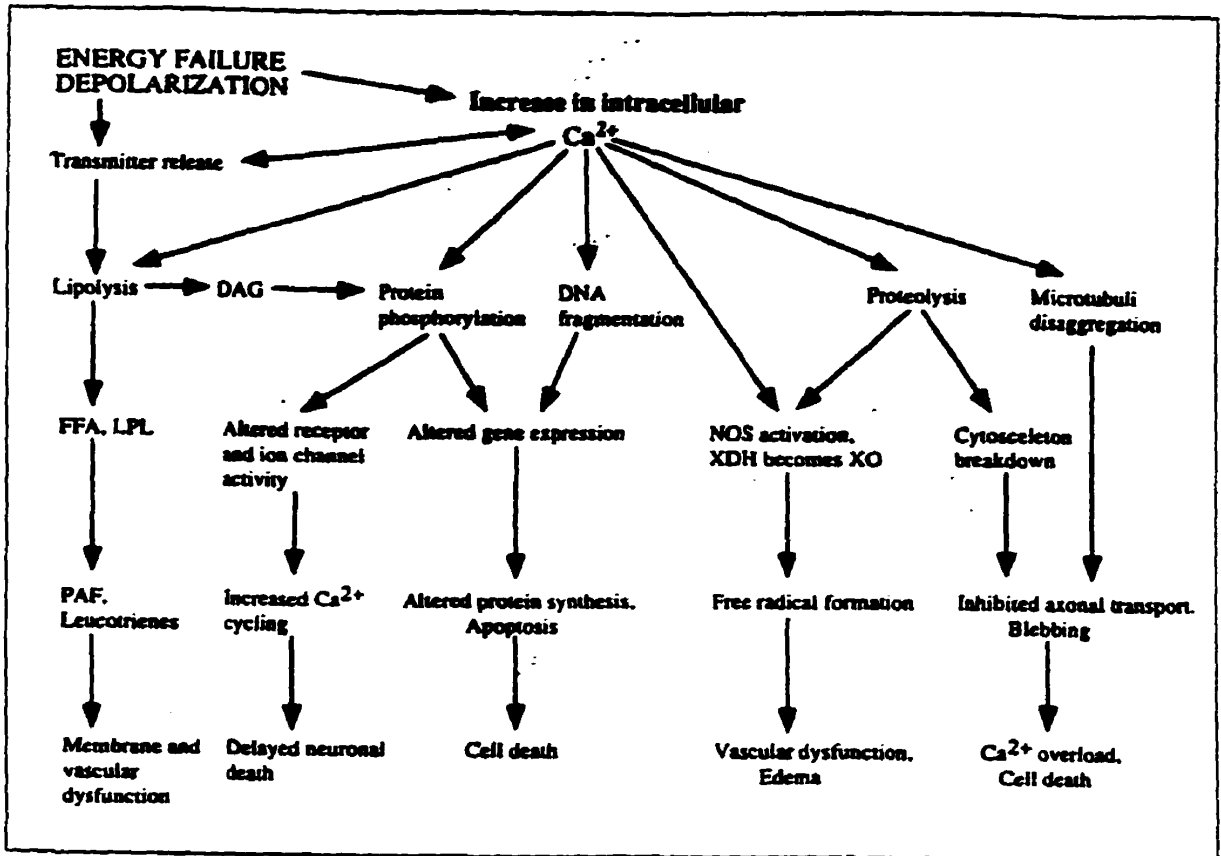
these glutamate receptor subtypes have been shown to produce excitotoxic cell death in a similar way to that observed with glutamate alone (Cai and Erdo, 1992; Koh et. al., 1990) e.g NMDA, Kainic acid, Quisqualic acid, and AMPA. The role of the non-NMDA receptor subtypes-AMPA and Kainate, have also become more evident in neuronal ischemia and/or anoxia. Until recently, it was widely accepted that KA and AMPA activate intrinsic  $\text{Na}^+$  and  $\text{K}^+$  channels, respectively; while NMDA activated a  $\text{Ca}^{2+}$  channel. However, recent studies have demonstrated that  $\text{Ca}^{2+}$  influx may be gated through both NMDA and KA channels (Keller et. al., 1992; Ozawa et. al., 1991). AMPA and KA were found to be more toxic than NMDA, Quinilinate, or Glutamate, both under normal conditions and energy depleted conditions. In fact, Schurr and Rigor (1993) show that the KA receptor is involved in the mechanism of neuronal damage induced by hypoxia and glucose deprivation, probably allowing  $\text{Ca}^{2+}$  influx and subsequent intracellular  $\text{Ca}^{2+}$  overload. In hypoxia, AMPA and KA appear to activate their own associated channels as well as the NMDA associated channels but under glucose deprivation, KA mainly activates its own receptors. The NMDA subtype glutamate receptor, however, is thought to play a more complex role in mechanisms of neuronal injury in response to oxygen and/or energy limitation, when compared with the non-glutamate subreceptors. Using organotypic hippocampal slice cultures, Pringle et. al. (1997) demonstrated that neuronal death following either hypoxia or ischemia was prevented by either pre-incubation or post-insult with various NMDA receptor antagonists. Neuroprotection by non-NMDA and NMDA channel antagonists suggests that a concurrent activation of both channel types is required for the initiation of neuronal damage during anoxic and ischemic treatments. The authors proposed that activation of non-NMDA receptors opens a receptor-linked ion channel with a high  $\text{Na}^+$  and low  $\text{Ca}^{2+}$  conductance.



Increased  $\text{Na}^+$  influx across the cell membrane via AMPA channels could cause the anoxic depolarization that is characteristic of ischemic insult. One consequence of this will be the removal of the  $\text{Mg}^{2+}$  block of the NMDA channel resulting in NMDA mediated damage (Choi, 1990). Bickler and Hansen (1994) studied the influence of antagonists of NMDA and AMPA on the rise in  $[\text{Ca}^{2+}]_i$ , and concluded that during ischemia, combined antagonism of all three channel types slowed the rate of  $[\text{Ca}^{2+}]_i$  accumulation. They proposed that the sustained elevation in cytosolic  $\text{Ca}^{2+}$  caused by ischemic stress is dependent on the concurrent activation of both NMDA and AMPA channels. Thus, massive release of glutamate into the extracellular space initiates a wave of neuronal death through cellular depolarization and destruction of ionic homeostasis, creating cellular excitotoxicity. The explosive rise in intracellular  $\text{Ca}^{2+}$  has been implicated in triggering various cellular dysfunction effects: DNA fragmentation, proteolysis, altered gene expression, altered receptor and ion channel activity, apoptosis, free radical formation and cytoskeletal breakdown (Fig. 4). These events result in the collapse of cellular membrane and vascular integrity, creating excitotoxicity in the neighbouring neurons. In this manner, the anoxic wave of destruction spreads to all parts of the vulnerable mammalian brain.

Based on the information presented, anoxia/ischemia induced cell death most likely occurs via the following sequence of events: decreased ATP levels, an initial  $\text{K}^+$  efflux through  $\text{K}^+_{\text{ATP}}$  channels setting the stage for anoxic depolarization, a concomitant activation of various  $\text{K}^+$ ,  $\text{Na}^+$  and  $\text{Ca}^{2+}$  permeable channels resulting in the disruption of transmembrane ionic gradients and cellular depolarization, increases in intracellular  $\text{Ca}^{2+}$  leading to irreversible cellular excitotoxicity and subsequent cell death.

**Fig. 4.** Overview of the postulated mechanisms by which a rise in intracellular  $\text{Ca}^{2+}$  jeopardises neuronal survival during and after anoxic/ischemic damage. Note the interrelationships indicated between several of the potentially deadly mechanisms which include lipolysis, neurotransmitter release, apoptosis and free radical formation. (DAG=diacylglycerides; FFA=free fatty acids; LPL=lysophospholipids; NOS=nitric oxide synthase; PAF=platelet activating factor; XDH=xanthine dehydrogenase; XO=xanthine oxidase). Reprinted from Lutz and Nilsson (1997).



## THE TURTLE BRAIN: A MODEL OF ANOXIA TOLERANCE

In striking contrast to the anoxia sensitive mammalian brain, the anoxic turtle brain can survive several weeks and even months of anoxia at low temperatures (Jackson and Heisler, 1984; Ultsch, 1985). Other anoxia tolerant species include the goldfish (*C. auratus*) and the crucian carp (*C. carassius*), known to survive 12 and 20h of anoxia, respectively (van der Boon et. al., 1992; Johansson et. al. 1995). Intertidal fishes and eels and tilapia show an intermediate tolerance to anoxia: the european eel (*Anguilla anguilla*) survives approximately 6h of anoxia at 15°C (Van Waarde et. al., 1983) and the tilapia species *Sarotherodon mossambicus* is able to tolerate anoxia for at least 2h at 20°C (Van Ginneken et. al., 1996).

It is important to establish that the exceptional anoxia tolerance of these species cannot be attributed simply to a lesser metabolic demand compared to that of the mammalian brain. A high obligatory rate of energy consumption is a problem which is common to all vertebrates when temperature is taken into account. The mass specific oxygen consumption rates of vertebrate brains are similar, ranging from approximately 80 to 200 $\mu\text{mol O}_2/\text{g}\cdot\text{h}$  in fish to mammals (Lutz and Nilsson, 1994). In fact, at the same temperature (31°C) rat and turtle brain synaptosomes consume identical amounts of oxygen with corresponding changes in the rate of oxygen consumption with  $\text{Na}^+$  channel activation and inactivation (Edwards et. al., 1989). Furthermore, Robin et. al (1979) found insignificant differences in rat and turtle brain slice oxygen consumption rates at 21°C. In the absence of glycolytic substrate, the anoxic turtle brain undergoes anoxic depolarization (AD) similar to that in the rat brain. In the turtle brain, inhibition of the glycolytic pathway with iodoacetate results in a neuronal  $\text{K}^+$  efflux (Sick et. al., 1982), a precursor event to a loss of ionic homeostasis and cell excitotoxicity. As with the rat brain, the anoxic turtle brain also undergoes metabolic

acidosis with the elevation of lactate and depletion of high energy metabolites such as phosphocreatine (PCr) and ATP (Chih et. al., 1989a; Lutz et. al., 1985). These studies suggest that there are fundamental mechanistic differences between the turtle and rat brain which confer anoxia tolerance to the former and not the latter.

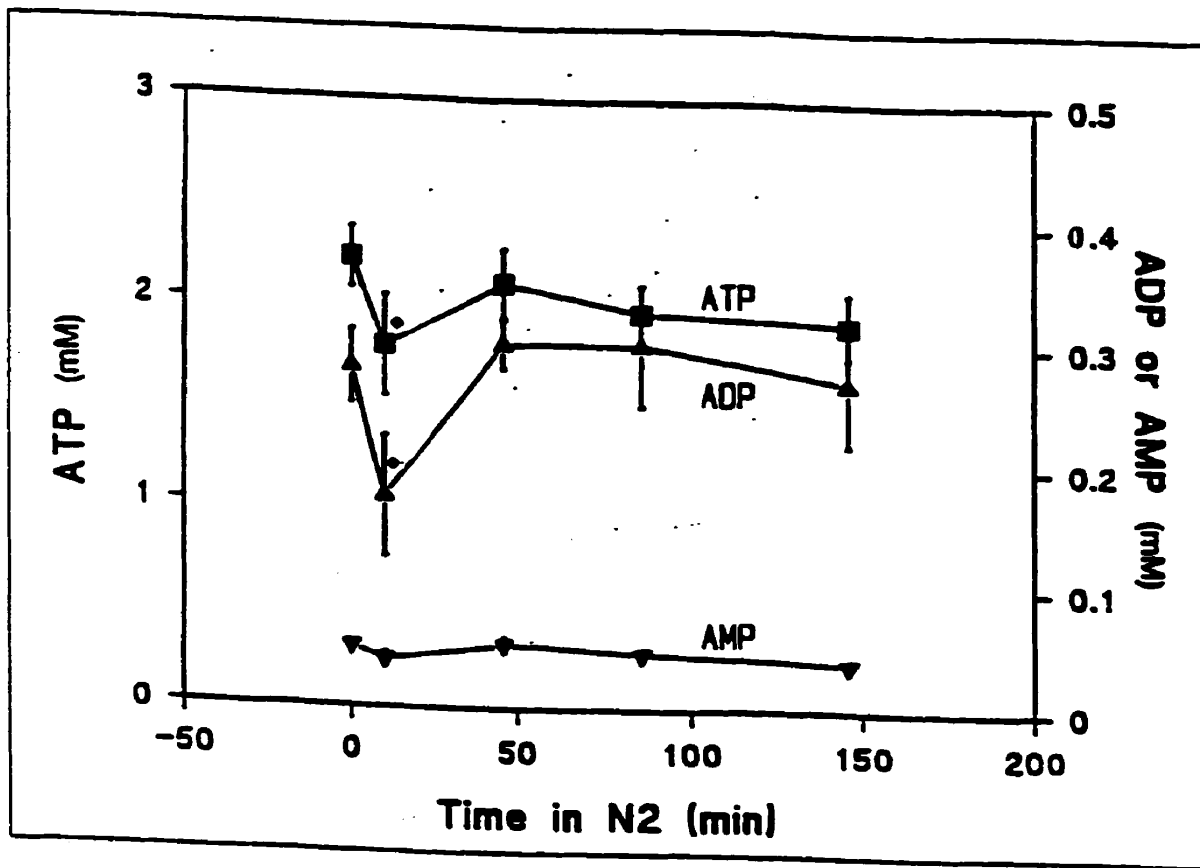
One must also take into account that anoxia tolerant brains are uncommon even among ectothermic vertebrates: the brains of lizards (*Angolis sagrei*) are much less anoxia tolerant than those of the turtle *T.scripta* (Nilsson et. al., 1991) and when corrected for temperature, the brain of the rainbow trout exhibits virtually identical susceptibility to anoxia when compared with the mammalian brain (Hylland et. al., 1995). There are also interspecies differences in anoxic survival times among turtles, with the western painted turtle (*Chrysemys picta belli*) surviving anoxia for up to 6 months whereas minimal viability is exhibited by the soft-shelled turtle *Sternotherus odoratus* (5.2 days) (Ultsch, 1985). From these studies, it is evident that anoxia tolerant vertebrate brains survive anoxia as a result of physiological adaptations that allow for the conservation of ATP and prevention of energy failure. Since a much reduced level of ATP produced from anaerobic glycolysis is the sole pathway of ATP production, the anoxic vertebrate brain must match its level of ATP utilization with ATP production in order to survive. Adaptive strategies which would allow for maintenance of ATP supply in the anoxic brain and confer anoxia tolerance include a reduction in metabolic rate along with a suppression of electrical activity and a reduction in basal cellular ion fluxes.

## **REDUCED GLYCOLYTIC ACTIVITY AND “METABOLIC ARREST”**

Several studies demonstrate a maintenance of energy status under both normoxic and prolonged anoxic conditions in the turtle brain. During the transition to anoxia, CrP levels are reduced to 50% of control within 20min of anoxia (Lutz, 1992). Furthermore, ATP and ADP levels initially decline in the anoxic turtle brain (Chih et. al., 1989a) but begin to increase again due to increases in the glycolytic activity of the turtle brain as indicated by elevated lactate levels (Lutz et. al., 1985), activation of pyruvate kinase (Kelly and Storey, 1988), and constant heat production despite the fall in oxygen consumption (Perez-Pinzon et. al., 1992b). Anoxic turtle brain ATP levels return to aerobic levels and remain constant thereafter for up to 5h of anoxia (Fig. 5) (Lutz et. al., 1984; Perez-Pinzon et. al., 1992b). The crucian carp and goldfish also maintain brain ATP levels for at least 20h at 12°C (Johansson et. al., 1995) and for 12h anoxia at 20°C (van der Boon et. al., 1992) respectively. However, the increase in the glycolytic capacity observed in the turtle brain upon anoxic insult is only temporary as supported by a drastically reduced turtle brain glycolytic rate during prolonged anoxia (Lutz et. al., 1984).

Support for a lowered glycolytic enzyme activity comes from Brooks and Storey (1988) who have demonstrated that covalent modification of key regulatory glycolytic enzymes (glycogen phosphorylase, phosphofructokinase) produces less active forms in anoxic turtle organs. Furthermore, from a crossover analysis of changes in the concentration of glycolytic intermediates in normoxic and anoxic turtle brain, Kelly and Storey (1988) have also shown that glycolytic rate is depressed in the turtle brain after 1h of anoxic exposure at 18°C. These studies suggest that ATP levels continue to be maintained in the turtle brain

**Fig. 5. Changes in the brain levels of ATP, ADP, and AMP during N<sub>2</sub> respiration in the freshwater turtle. Adapted from Lutz et. al. (1984).**



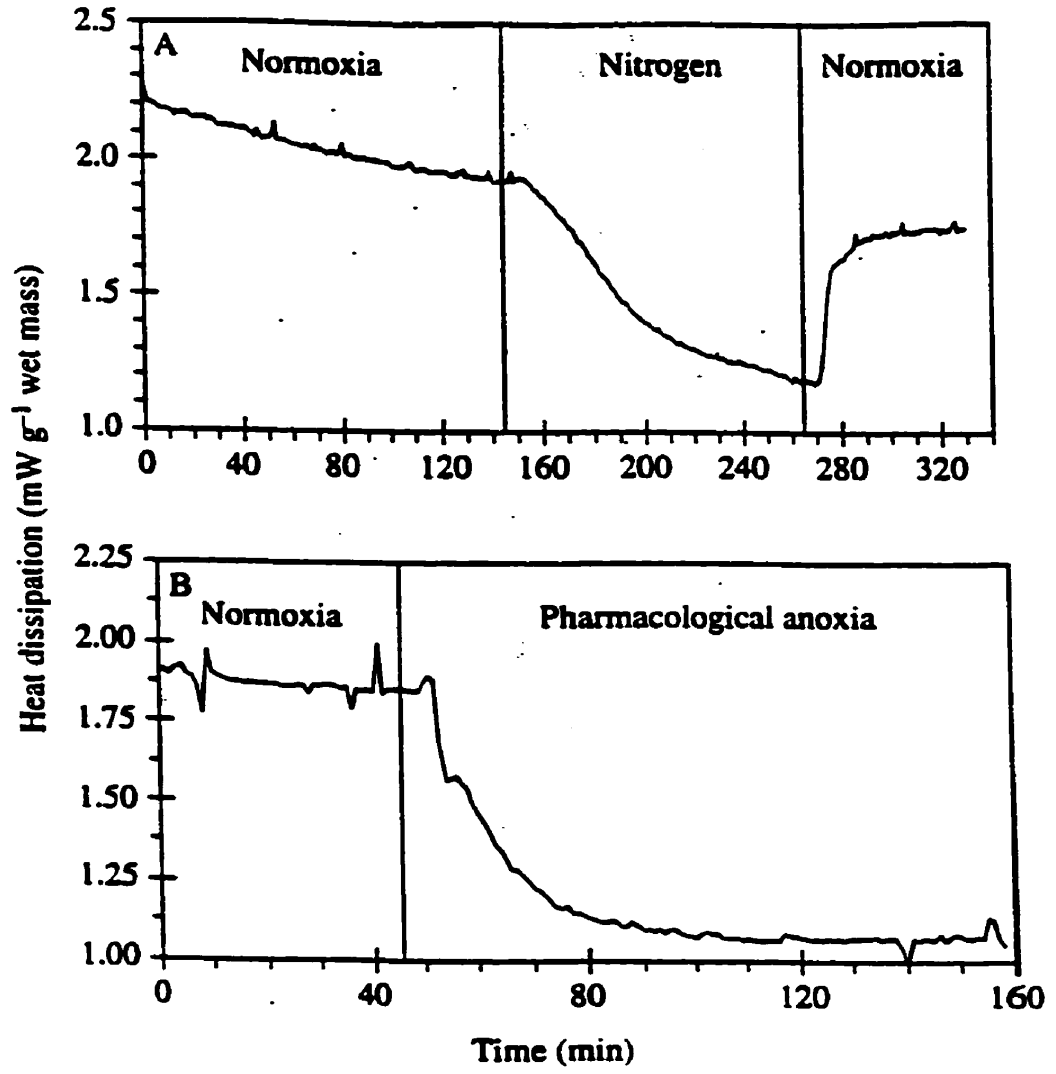


eventhough the glycolytic rate is drastically reduced during prolonged anoxia. A potential mechanism to explain this phenomenon involves a reduction in the overall metabolic rate of the turtle, thus enabling anaerobic glycolysis to better meet the energy demand in the anoxic turtle brain.

Brain hypometabolism is fundamental to the survival of the turtle during anoxia. Since glycogen depletion is the only factor that limits survival of the anoxic turtle, then a reduction in the metabolic rate would lead to reduced glycogen depletion rate and prolonged anoxia tolerance. Evidence for a reduced metabolic rate, or “metabolic arrest”, in the anoxic turtle comes from whole body calorimetric studies which indicate that heat production falls to 25% of control within 2h anoxia (Jackson, 1968). In the western painted turtle (*Chrysemys picta belli*), chronic anoxic submergence is accompanied by a 84-88% reduction in ATP demand both in the whole animal (Herbert and Jackson, 1985*b*; Robin et. al., 1964; Ultsch and Jackson (1982) and in isolated hepatocytes (Buck et. al., 1993*a, b*).

With respect to the turtle brain, anoxia produces a 40% reduction in the metabolic rate of isolated brain slices as suggested by calorimetry studies (Perez-Pinzon et. al., 1991). Furthermore, direct calorimetry of cortical slices supports a 50% reduction in heat production with anoxic exposure (Fig. 6), the overall metabolic suppression in the turtle brain being about 50% of normoxic rates (Doll et. al., 1994). To achieve “metabolic arrest”, energy consuming processes such as Na<sup>-</sup> pump, urea synthesis, and gluconeogenesis have been shown to be significantly suppressed in the anoxic turtle when compared to normoxic controls (Buck et. al., 1993*b*; Land et. al., 1993). Additionally, Land et. al. (1993) have demonstrated that turtle hepatocyte protein synthesis and the ATP utilized specifically for

**Fig. 6.** Representative chart drawings of heat dissipation during (A) nitrogen perfusion and (B) pharmacological anoxia for turtle cortical slices (25°C). Vertical lines indicate the time at which the indicated solution entered the calorimeter slice chamber. Reprinted from Doll et. al. (1994).



this process was reversibly reduced by 92% under anoxia with normoxic recovery resulting in a 160% increase in protein synthesis rates compared to control. Similarly, ATP dependent protein degradation through proteolysis was also depressed significantly (93%) in isolated turtle hepatocytes (Land and Hochachka, 1994).

An alternative pathway to induce “metabolic arrest” in anoxia tolerant species involves the action of Gamma-aminobutyric acid (GABA). In both the crucian carp and the turtle brain, tissue concentrations of GABA increase during anoxia (Nilsson, 1990; Nilsson et. al., 1990). Nilsson (1992) has shown that the systemic metabolic rate of anoxic crucian carp is greatly increased during anoxia by antagonists of GABA<sub>A</sub> receptors. Furthermore, extracellular levels of GABA also increase in the anoxic turtle brain (Nilsson and Lutz, 1991). GABA<sub>A</sub> receptors have also been found to be upregulated in the turtle brain (29% after 24hrs anoxia) during anoxia (Lutz and Leone-Kabler, 1995). GABA release is thought to be important in triggering the efflux of HCO<sub>3</sub><sup>-</sup> from the cell (Kaila and Voipio, 1987) thus reducing intracellular pH. An increase in the acidity of the cell would inhibit enzyme activity, thus depressing metabolism (Trivedi and Danforth, 1966). Taken together, increased levels of GABA and the upregulation of GABA<sub>A</sub> receptors may serve to increase the effectiveness of this neurotransmitter in inducing metabolic arrest in the anoxia tolerant brain. From the studies discussed, “metabolic arrest” is a key strategy utilized by the turtle brain to survive anoxia.

It is evident that an overall reduction in the rate of ATP production during anoxia is useful in lowering substrate use and the build-up of toxic endproducts. However, a reduction in ATP production is of little use without a concomitant reduction in the rate of ATP

utilization of various metabolic processes. An example of one such ATP consuming activity is the maintenance of cellular ionic gradients.

### **“CHANNEL ARREST” AND “SPIKE ARREST” CONTRIBUTE TO METABOLIC DEPRESSION IN THE ANOXIC TURTLE BRAIN**

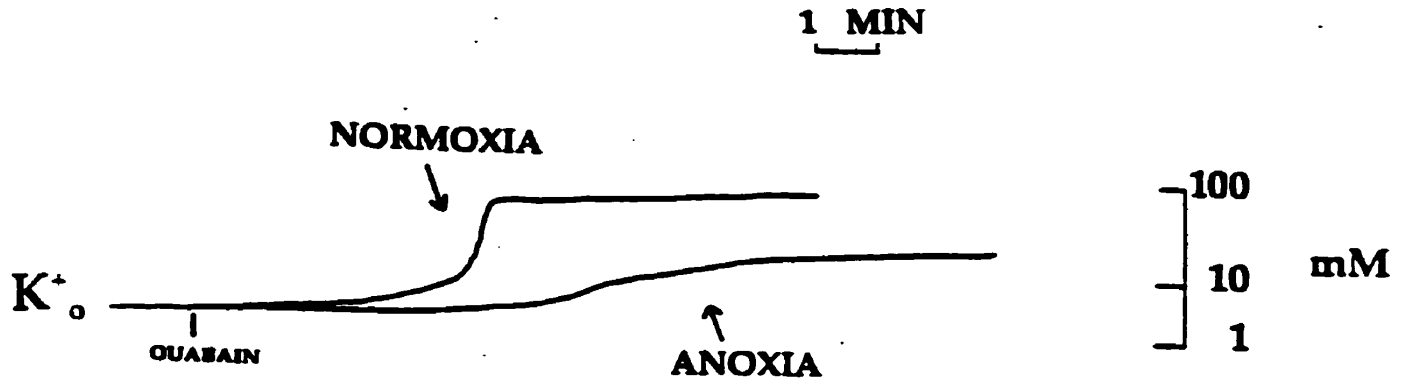
Transmembrane ion movement occurs in all cells. Cellular processes which contribute to transmembrane ion movement are activation of voltage gated and ligand gated ion channels resulting from electrical activity, NT release and uptake, co- and counter transport systems, and voltage-independent leakage channels (Hille, 1992). Whether ionic currents occur because of ion leakage, action potentials, or receptor activation, the ions have shifted position across the cell membrane and must be restored to their original compartment to maintain transcellular ionic gradients. The maintenance of ionic gradients under requires continual ion pumping through the use of ATP-consuming pumps, such as  $\text{Na}^+/\text{K}^+$  ATPase. This pump alone can consume approximately 50% of a cell's total energy budget (McBride and Milligan, 1985). Thus, any changes in turtle membrane physiology that would reduce the amount of ATP utilized by the  $\text{Na}^+/\text{K}^+$  pump would offer unique advantages to spare energy for cell survival during anoxia. One possible mechanism to achieve this is to reduce cell membrane ion permeability.

In fact, a mechanism of this sort has been proposed: it is called the “Channel Arrest” hypothesis and it predicts that anoxia tolerant species reduce their cellular ion permeability to reduce ion pumping, thus conserving ATP that would ordinarily be consumed for this purpose (Hochachka, 1986). A similar hypothesis proposed by Chih et. al. (1989b) states that ion pumping may also be reduced through a reduction or suppression of turtle brain electrical activity, termed “Spike Arrest”. A reduction in electrical activity may be brought about by

inhibiting channel activity associated with action potentials or by reducing their activity by suppressing synaptic transmission (Lutz and Nilsson, 1997). Indeed, the evidence discussed below strongly suggests a reduction in the permeability of several ion species, mediated in part by adenosine, resulting in depressed electrical activity in the anoxic turtle brain.

***K<sup>+</sup> channels:*** In the mammalian brain, anoxia produces a rapid fall in ATP, which causes ATP-dependent activities (ATPase) to fail, resulting in an increase in extracellular K<sup>+</sup>. This increase in extracellular K<sup>+</sup> causes membrane depolarization which ultimately results in the death of the cell from uncontrolled increases in cytosolic Ca<sup>2+</sup>. In contrast to the mammalian brain, the anoxic turtle brain does not undergo a K<sup>+</sup> efflux. In the intact turtle brain, [K<sup>+</sup>]<sub>o</sub> is stable throughout 6 hours of anoxia (Feng et. al., 1988). Using autoradiographic techniques, Xia and Haddad (1993) found a differential distribution of K<sub>ATP</sub> channels in the adult and newborn rat brain, and the turtle brain. The authors found a striking heterogeneity in the distribution and density of sulfonylurea receptors in the adult rat CNS and this is in sharp contrast to the homogenous distribution and low density in both newborn rat and adult turtle. It is speculated that K<sub>ATP</sub> channels are poorly developed in the newborn rat and adult turtle, developing mostly after birth in the rat, reaching highest density in adulthood. This decreased density of K<sub>ATP</sub> channels may contribute to the lower K<sup>+</sup> efflux observed in the anoxic turtle brain. However, it has been demonstrated that the rate of K<sup>+</sup> efflux in ouabain (Na<sup>+</sup>/K<sup>+</sup> ATPase inhibitor) treated brains is substantially less during anoxia in the turtle (Pek and Lutz, 1997) when compared to normoxic controls. Using extracellular electrodes, another study compared the rate of K<sup>+</sup> leakage in the anoxic and normoxic turtle brain and found that the rates of K<sup>+</sup> leakage were significantly lower in brains subjected to anoxia than in normoxic brains (Fig. 7) (Chih et. al., 1989b). These studies suggest that ion channels are

**Fig. 7.** Changes in extracellular  $K^+$  ( $K^+_o$ ) in normoxic and anoxic turtle brains during superfusion of brains with 10mM ouabain. For the anoxic experiment, animal was respired with  $N_2$  for 2h before ouabain superfusion. Reprinted from Chih et. al. (1989*b*).





actively regulated to reduce ion leakage and may constitute an important mechanism to conserve ATP in the anoxic turtle brain.

***Na<sup>+</sup> Channels:*** In the anoxic turtle brain, brain electrical activity is depressed but not suppressed with a reduction in evoked potentials to about 20-50% of normoxic levels during anoxia (Feng et. al., 1988) with rapid recovery of evoked potential activity upon oxygenation (Perez-Pinzon et. al., 1992a). A similar reduction in electrical activity is also observed in the goldfish, where anoxia causes a strong suppression of sound-evoked electrical activity, changes which reflect a lowered presynaptic activity (Suzue et. al., 1987; Fay et. al., 1992).

In the Purkinje cells of the turtle cerebellum, sodium spike thresholds are increased and postsynaptic responses from major afferent input pathways to the purkinje cells are depressed during anoxia (Perez-Pinzon et. al., 1992a). Increased Na<sup>+</sup> spike thresholds implies that, postsynaptically, it should be more difficult to provoke sodium spike responses and presynaptic calcium (dendritic) spikes should be less effective in promoting sodium spike activity. The overall result would be decreased electrical activity in purkinje cells. The authors have suggested that one possible mechanism for elevating Na<sup>+</sup> spike threshold is the down regulation of Na<sup>+</sup> channels by channel inactivators. Support for this mechanism comes from a study which reports that anoxia induces a significant (42%) decrease in voltage gated Na<sup>+</sup> channel density as determined by sodium channel ligand binding (Brevetoxin[<sup>3</sup>H]) (Perez-Pinzon et. al., 1992c). Furthermore, Edwards et. al. (1989) found in a turtle synaptosome preparation that there were 67% fewer binding sites than in rat brain synaptosomes, suggesting that the turtle synaptosomes have a lower Na<sup>+</sup> channel density than the rat. Thus, it is possible that downregulation of Na<sup>+</sup> channels may be the basis for shifts in

action potential thresholds, electrical depression and decreases in ion flux that could relieve the energetic costs associated with maintaining ionic gradients across the cell membrane.

***Ca<sup>2+</sup> Channels:*** In comparison to what is currently known about the action of voltage gated and receptor gated channels in mediating Ca<sup>2+</sup> flux in the rat brain during energy limitation, very little evidence is presently available with regard to the same action in the turtle brain. Significant reductions in glutamate mediated calcium fluxes have been demonstrated in the turtle brain after 14h of anoxia (Bickler and Galego, 1993). Similarly, Buck and Bickler (1995) have shown that cortical slices exposed to anoxia exhibit a 52% decrease in the NMDA-mediated [Ca<sup>2+</sup>] rise, from 232±30 to 111±9nM. A long term reduction in NMDA receptor activity in the anoxic turtle cerebrocortex has also been demonstrated (Bickler, 1998). In a direct measure of channel arrest NMDA receptor open probability has been shown to decrease by 65% in response to anoxia (Buck and Bickler, 1998), suggesting that reductions in glycolytic ATP production during anoxia are matched with corresponding decreases in Ca<sup>2+</sup> channel activity, thus effectively maintaining a coupling between membrane ion homeostasis and ATP production.

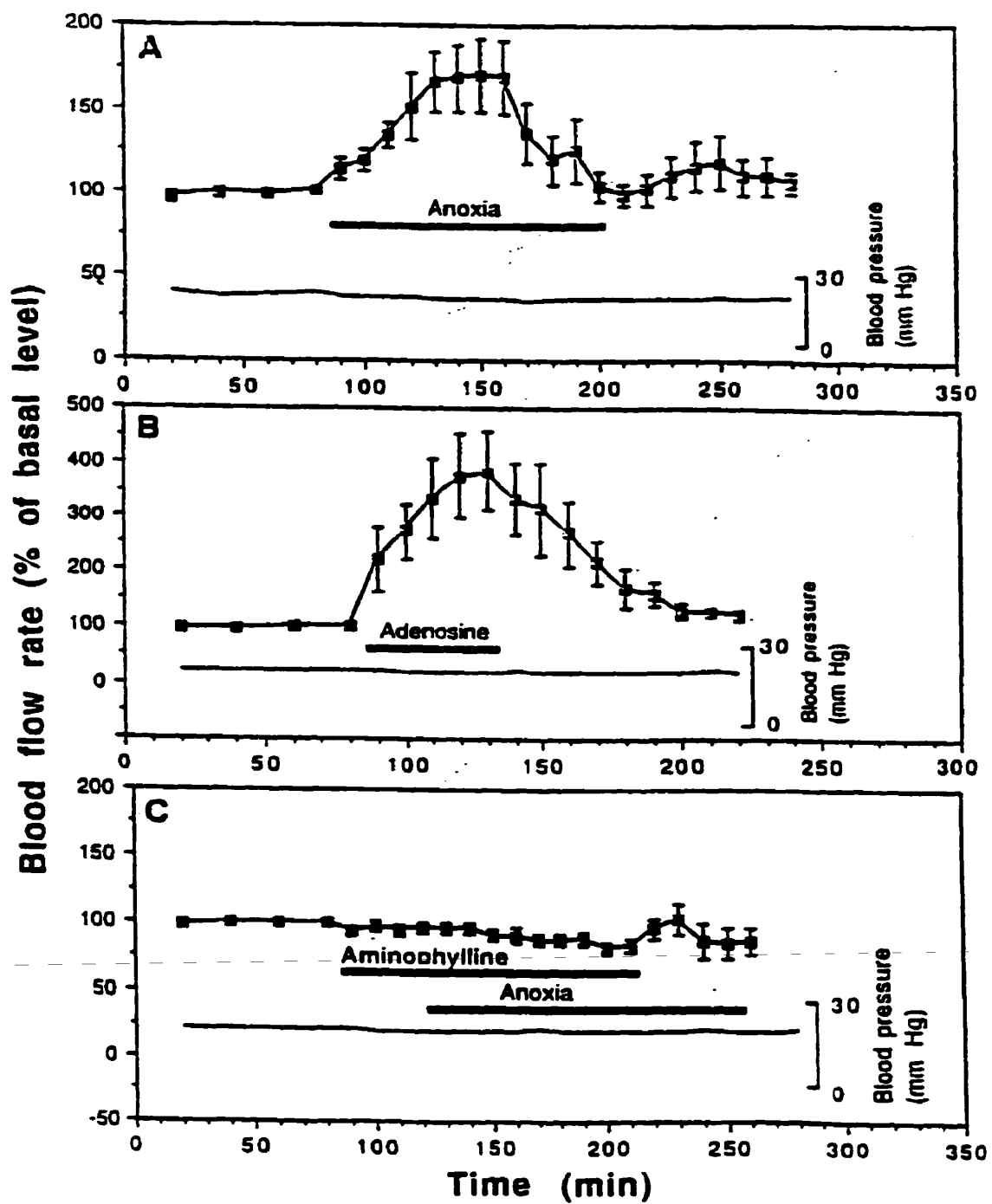
***Adenosine:*** Adenosine is considered to play an important neuroprotective role during the transition to anoxia in the turtle brain and may be important in promoting channel and spike arrest. In the turtle, shortly after the onset of brain anoxia there is a substantial rise in extracellular adenosine (Nilsson and Lutz, 1992). Adenosine is known to increase blood flow to the anoxic brain, stimulate glycogenolysis and decrease brain electrical and synaptic activity (Newby et. al, 1990). These observations suggest that during anoxia, adenosine acts to increase the flow of nutrients to the energy deficient brain and reduces neuronal electrical

activity in an effort to reduce the amount of ATP the brain utilizes to re-establish neuronal ion gradients.

An adenosine mediated anoxia tolerance is supported by a finding which shows that superfusing the anoxic turtle brain *in situ* with the adenosine receptor blocker aminophylline prevents the (normal) anoxia-induced increase in brain blood flow (Fig. 8) (Hylland et. al., 1994). Furthermore, superfusing the anoxic isolated turtle cerebellum with the adenosine receptor blocker theophylline or 8-CPT causes a rapid depolarization which is a prelude to anoxic brain failure in mammals (Perez-Pinzon et. al., 1993). Evidence supporting the notion that adenosine may be part of a mechanism which regulates ion channel permeability is as follows: application of an A<sub>1</sub> receptor antagonist elicits the release of intracellular K<sup>+</sup> in the isolated turtle cerebrum during anoxia, the absence of such release being characteristic of anoxia tolerance in the turtle brain (Perez-Pinzon et. al., 1993); adenosine reduces the NMDA-mediated rise in intracellular [Ca<sup>2+</sup>] ([Ca<sup>2+</sup>]<sub>i</sub>) by 62% (Buck and Bickler, 1995) and reduces NMDA receptor open probability by 65% in the turtle cortex (Buck and Bickler, 1998).

The evidence presented supports the notion of “channel” and “spike arrest” as plausible defence mechanisms utilized by the anoxic turtle brain to survive both short and long-term anoxia. Furthermore, it is likely that adenosine works in concert with these mechanisms, functioning as a “retaliatory metabolite” by reducing energy consumption and increasing energy supply to the brain during anoxia. In summary, the turtle brain is thought to survive anoxia by maintaining a bioenergetic balance through changes in its

**Fig. 8.** Anoxia and adenosine cause increased brain blood flow in turtles exposed to anoxia. Note that both exposure to **(A)** anoxia and **(B)** adenosine induce increased blood flow rate and that **(C)** the anoxic increase in flow rate can be completely blocked by aminophylline-an adenosine receptor antagonist. Also note that the increased blood flow rate during anoxia is only temporary. Blood flow rate was measured with epi-illumination microscopy *in vivo*. Adenosine and aminophylline was administered topically, blood pressure was measured systemically (subclavian artery). From Hylland et. al. (1994).



physiology which allow for reductions in energy demand to a level that can be satisfied through anaerobic glycolytic ATP production. Adaptive strategies which allow for this include (i) metabolic arrest with an accompanying decrease in glycolytic rate and (ii) an overall decrease in membrane permeability (channel arrest) resulting in depressed neuronal electrical activity (spike arrest).

## RESEARCH PROPOSAL

### ***HYPOTHESIS 1: DOES WHOLE CELL PERMEABILITY CHANGE IN THE ANOXIC TURTLE BRAIN?***

The western painted turtle is the most anoxia tolerant vertebrate presently known, surviving as long as 6 months of anoxia at low temperature (Ultsch, 1985). The most effective strategy employed by such a species to survive long-term anoxia is probably the coordinated suppression of ATP utilizing and producing pathways. The anoxic turtle brain still maintains ionic gradients, actively pumps ions (Sick et. al., 1982), and is electrically active although at a reduced level (Feng et. al., 1988b).

A hypothesis that can account for such alterations is the "channel arrest" hypothesis (Hochachka, 1986) which predicts that: 1) in hypoxia tolerant species the plasma membrane ought to be less permeable to ions than intolerant species, and 2) tolerant species ought to have mechanisms to acutely regulate cellular ion permeability. A previous whole cell voltage clamp study tested the second aspect of this hypothesis and found no significant changes in whole cell conductance in response to anoxia in a turtle brain slice preparation (Doll et. al., 1991, 1993b). However, this study was conducted using high resistance electrodes (30-70 M $\Omega$ ) which may be unable to achieve an effective whole cell clamp configuration and was thus unable to accurately measure any change in whole cell conductance. Furthermore, high levels of the calcium ion chelator ethylene glycol-bis( $\beta$ -aminoethyl ether) N,N,N',N'-tetraacetic acid (EGTA) were used in the recording electrode and if changes in  $[Ca^{2+}]_i$  are an important event mediating the cellular response to anoxia, then any change would have been buffered by the presence of EGTA.

I tested the 2<sup>nd</sup> aspect of the “channel arrest” hypothesis using the anoxia tolerant turtle (*Chrysemys picta belli*) as a model system. To accomplish this, I repeated the experiments conducted by Doll et. al. (1991) using lower resistance whole-cell patch electrodes (6-8 M $\Omega$ ) and EGTA-free recording electrode solutions to determine whether a change in whole cell conductance occurs in anoxic turtle brain sheets. Furthermore, since turtle blood concentrations of Ca<sup>2+</sup>, Mg<sup>2+</sup>, and H<sup>+</sup> have been shown to increase greatly in a dived turtle (Herbert and Jackson, 1985a) I also examined the effect of an acute perfusion of a “mimic” aCSF consisting of Ca<sup>2+</sup>, Mg<sup>2+</sup> concentrations, and low pH on whole cell conductance. Finally, the effect of adenosine on whole cell conductance was also studied to test the involvement of a second messenger pathway.

***HYPOTHESIS 2: ARE GAP JUNCTIONS INVOLVED IN MODULATING WHOLE  
CELL PERMEABILITY IN THE ANOXIC TURTLE BRAIN?***

Any changes in whole cell conductance can be attributed to changes in individual ion channel properties or to changes in gap junction permeability. Gap junctions provide electrical continuity among various cell types in both invertebrate and vertebrate nervous systems (Jeffreys, 1995). Gap junction channels are composed of 12 subunits (connexin proteins), six of which are contributed by each of the coupled cells to form hemichannels (connexons). Gap junctions provide extensive coupling among glia in the turtle dorsal cortex (Connors and Ransom, 1987) and have been studied extensively in various rodent brain models using dye-coupling (MacVicar and Dudek, 1981) and freeze-fracture preparations (Shiosaka et. al., 1989). Experimental evidence suggests that gap junctions can be modulated functionally in response to the neurotransmitter application (Hampson et. al., 1992, 1994),



and second messenger action (Kandler and Katz, 1995). Therefore, it is possible that induction of anoxia triggers a series of second messenger cascades which close gap junctions and decrease whole cell conductance.

I therefore used a whole-cell patch clamp technique to measure whole-cell capacitance in turtle cortical sheets during normoxic, anoxic, high adenosine (200 $\mu$ M) and high Ca<sup>2+</sup> (4mM) perfusions. Furthermore, I have performed dye-coupling studies with Lucifer yellow filled-patch electrodes to determine whether dye propagation to neighbouring cells occurs in either normoxic or anoxic cortical sheets.

## MATERIALS AND METHODS

### ANIMALS:

These studies were approved by the University of Toronto Animal Care committee, and conform to relevant guidelines for the care of experimental animals. Spring, summer and autumn female turtles (*Chrysemys picta belli*, Snelder) weighing between 250 and 500 g were obtained from Lemberger, Oshkosh, WI, USA. Animals were housed in a large aquarium equipped with a flow-through dechlorinated fresh water system at 23°C, basking platform and lamp. Turtles were maintained on a 12hr light/12hr dark photoperiod and given continuous access to food and water.

### DISSECTION AND EXPERIMENTAL CONFIGURATION:

Cortical brain sheets were prepared after decapitation and rapid removal of the cranium. The entire cerebral cortex was dissected free and placed in artificial turtle cerebrospinal fluid at 3-5°C (aCSF, in mM: 97 NaCl, 26.5 NaHCO<sub>3</sub>, 2.0 NaH<sub>2</sub>PO<sub>4</sub>, 2.6 KCl, 2.5 CaCl<sub>2</sub>, 2.0 MgCl<sub>2</sub>, 20 glucose and HEPES, pH 7.4 at 23°C). Individual cortical sheets (6-8 in total) were cut from larger cortical sheets as described by Blanton et al. (1989). All bathing and electrode filling solution osmolarities were measured with a vapour pressure osmometer (Wescor Model 5500) and adjusted to approximately 280mOsm.

Cortical sheets were supported by nylon mesh and held in place by a coil of platinum wire in a tissue slice recording chamber (Fine Science Tools Inc.). Conductance and capacitance recordings in the “whole cell” configuration were obtained from submerged and perfused cortical sheets (aCSF at 2-3 ml/min, 23°C). The tissue slice chamber was gravity

perfused from two 1 litre glass bottles with IV drippers and thick walled low gas permeability tubing. A three way stop cock and a pinch clamp were used to switch between IV bottles and regulate flow. Plastic tubing and IV drippers for anoxic experiments were double jacketed; N<sub>2</sub> gas was blown through the outer jacket to prevent O<sub>2</sub> from diffusing into perfusion solutions. The switching valve was as close as possible to the perfusion chamber, the measured line volume between switch and chamber was 1 ml and chamber volume 1.3 ml.

#### **WHOLE CELL CONDUCTANCE AND CAPACITANCE MEASUREMENTS:**

Whole-cell recordings were performed using the whole-cell voltage-clamp method with 6-8M $\Omega$  electrodes containing a recording solution which consisted of (in mM): 8 NaCl, 0.1 CaCl<sub>2</sub>, 5 EGTA, 10 HEPES Na, 20 KCl, 110 KOH, 1 MgCl<sub>2</sub>, 0.3 NaGTP, 2 MgATP, pH 7.4, adjusted with methanesulfonic acid. For some experiments EGTA was removed from the recording solution and Ca<sup>2+</sup> was adjusted to 1nM. This did not have a significant effect on osmolarity, remaining at approximately 280mosmol. Cell-attached 5 to 20 G $\Omega$  seals were obtained using the blind patch technique of Blanton et al. (1989). To break into a cell, the recording electrode potential was set at -60mV and a sharp pulse of suction was applied. Once the whole-cell configuration had been established, capacitance transients were removed using the capacitance compensation circuit of the Axopatch 1D, and access resistance was measured (ranging from 100 to 200M $\Omega$ ). From the voltage-clamp configuration, the Axopatch 1D amplifier was switched to the zero-current position and the membrane potential was read off the main meter. The whole cell configuration was allowed to stabilise for 2 min before resting membrane potential was determined (ranging from -65 to -85mV). Data were

collected using an Axopatch-1D amplifier, CV-4 headstage and Digidata 1200 interface (Axon Instruments, Burlingame, CA, USA) digitised at 20kHz and stored on computer. All collected data was analysed via computer using Pclamp software (version 6.0, Axon Instruments, Burlingame, CA, USA) (Fig. 9A). To measure whole-cell conductance Clampex software was used to step voltage from -60 to -93mV in -3mV increments lasting 250ms. Current values were measured between 200 and 220ms to avoid any capacitance effects and a slope conductance (whole cell conductance) was determined from the resultant current/voltage relationship (Fig. 9B).

Whole cell capacitance was measured using Clampex software to step voltage from -60 to -65mV in a single -5mV interval which lasted 7.5ms. The initial transient portion of the current response was integrated by the clampex software to determine the area under the transient curve ( $Q_t$ ) and a value for whole-cell capacitance was calculated using the algorithm,  $C_w = Q_t / \Delta V$  (Fig. 10).

**Fig. 9A.** A typical current response to a series of stepped voltages. Upon achieving a whole cell configuration, whole cell current responses were obtained by stepping neuronal membrane potential from -60 to -96 mV in 3 mV increments.

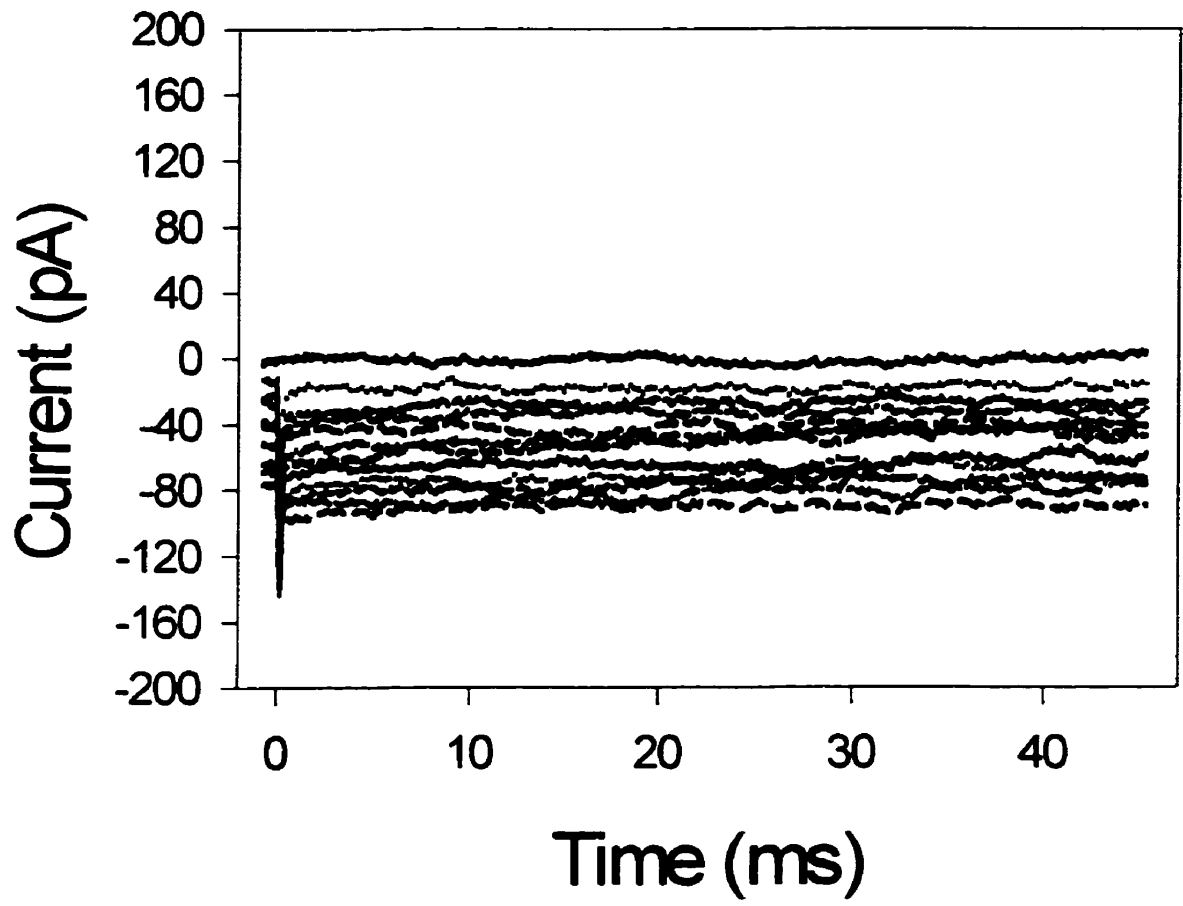


**Fig. 9B.** A typical current/voltage relationship obtained from data in the top panel. The slope of a regression of these data results in a slope conductance, or simply the whole-cell conductance, 2.65 nS.

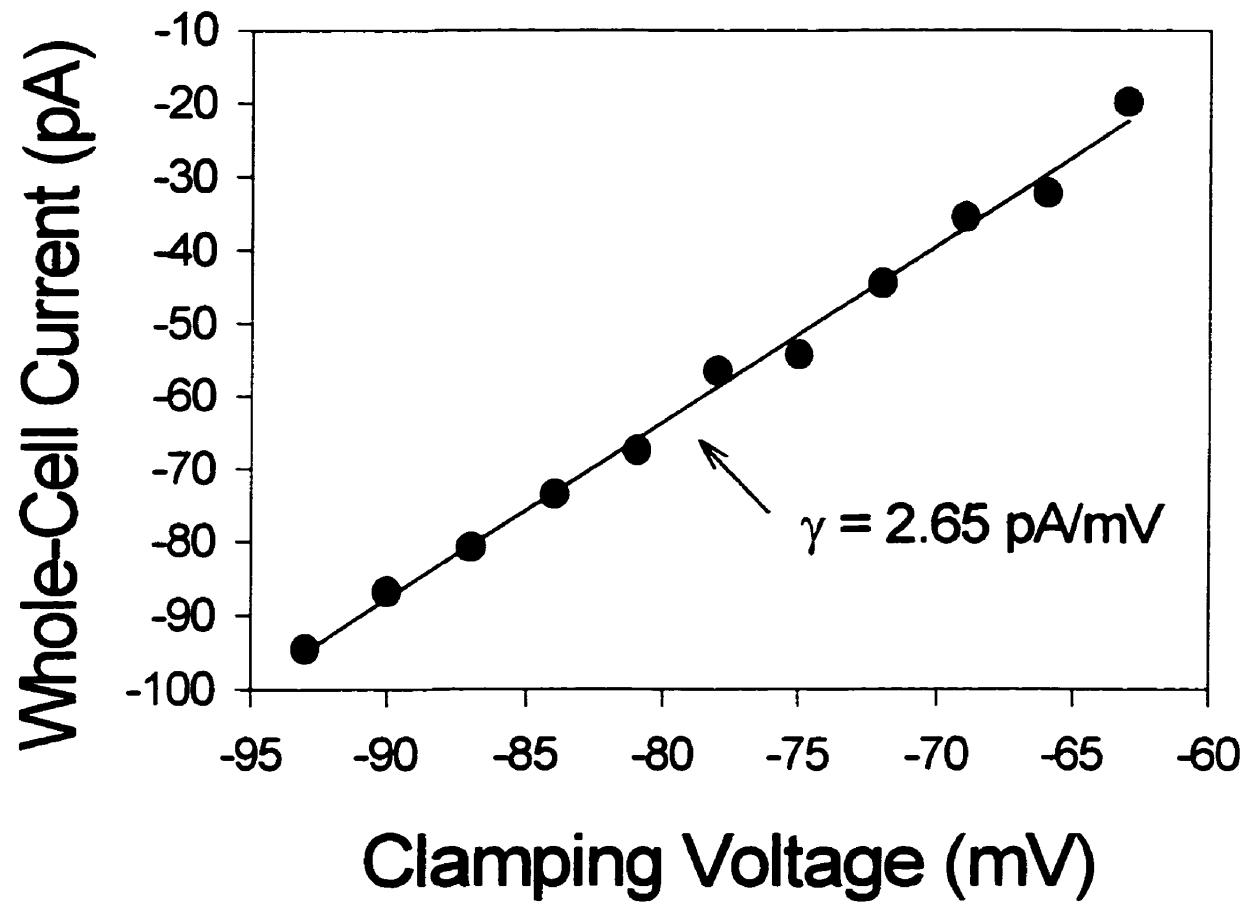
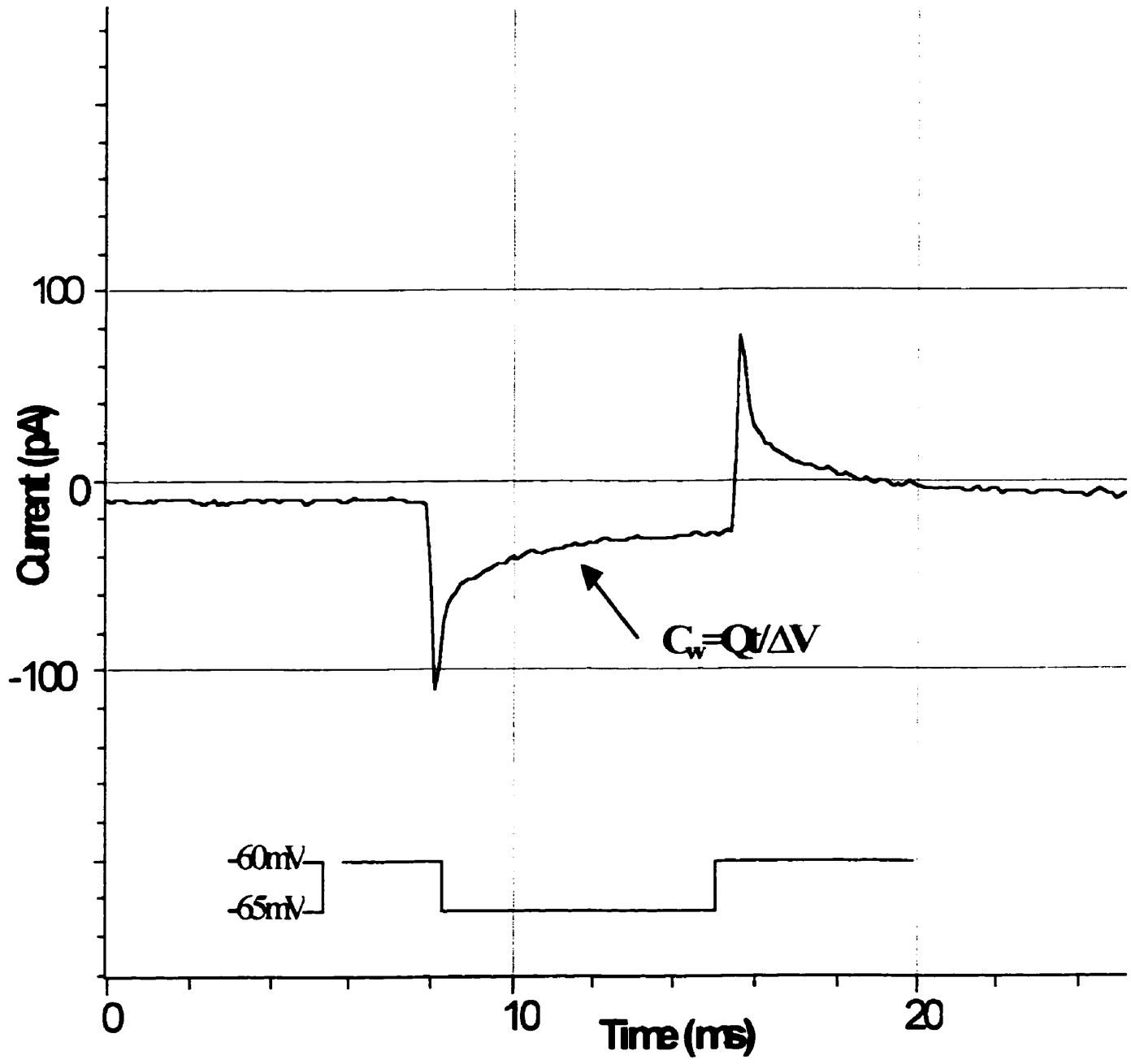




**Fig. 10. Whole cell capacitance response.** A typical current response to a step voltage from  $-60$  to  $-65\text{mV}$  in a single  $-5\text{mV}$  ( $\Delta V$ ) interval for a duration of  $7.5\text{ms}$ . A value for whole-cell capacitance is calculated using the algorithm,  $C_w = Q_t/\Delta V$ .  $Q_t$  is the area under the initial transient portion of the current response.



## WHOLE CELL CONDUCTANCE EXPERIMENTS

***Control and Anoxic Experiments.*** Experiments consisted of 130 or 70min time courses where 2 control points ( $t=0,10$ ) were obtained before a 60min treatment perfusion. Control experiments involved brain sheets perfused for 130min with normoxic aCSF with the inclusion of EGTA in the recording electrode. Control normoxic experiments were also conducted for 130min with the exclusion of EGTA from the recording electrode. For anoxic experiments the treatment reservoir was gassed with 95%N<sub>2</sub>/5%CO<sub>2</sub> and contained 0.5mM NaCN to prevent oxygenation artifacts. The recording chamber was fitted with a cap and a gas line allowing the chamber head space to be gassed with 95%N<sub>2</sub>/5%CO<sub>2</sub>. A small hole was made in the cap for the recording electrode to pass through and to vent positive gas pressure. Where recovery measurements were deemed useful, tissue was reperfused with normoxic aCSF for 60min. In sham experiments the patch clamp recording electrode was replaced with an oxygen electrode. When the perfusate and head space gas was switched from 95% O<sub>2</sub>/5% CO<sub>2</sub> to 95%N<sub>2</sub>/5%CO<sub>2</sub> the time required for aCSF P<sub>O2</sub> to drop below 1torr was 8 min.

***Mimic aCSF Experiments.*** "Mimic aCSF" composition was designed from values reported by Herbert and Jackson (1985a) and is (in mM): 97 NaCl, 26.5 NaHCO<sub>3</sub>, 2.0 NaH<sub>2</sub>PO<sub>4</sub>, 2.6 KCl, 7.8 CaCl<sub>2</sub>, 4.0 MgCl<sub>2</sub>, 20 glucose and 10 HEPES, pH 7.1 at 23°C). Cortical sheets were perfused with mimic aCSF containing 0.5mM NaCN and gassed with 95% N<sub>2</sub>/5%CO<sub>2</sub> to detect whether G<sub>w</sub> changes under conditions that mimic the composition of anoxic turtle blood. To determine if the mimic solution had effects on G<sub>w</sub> separate from those of anoxia alone a normoxic mimic experiment was carried out.

***Mg<sup>2+</sup> and pH Experiments.*** To determine if elevated levels of Mg<sup>2+</sup> and low pH had any effect on G<sub>w</sub>, cortical sheets were perfused with normoxic aCSF which contained either elevated levels of Mg<sup>2+</sup> (4.0mM) or low pH (7.1). Both sets of experiments were conducted in the absence of EGTA from the recording electrode

***Calcium Experiments.*** To determine if high extracellular Ca<sup>2+</sup> levels could have an effect on G<sub>w</sub>, cortical sheets were perfused with normoxic aCSF containing 4mM Ca<sup>2+</sup> in the absence of EGTA from the recording electrode. Additionally, in two separate sets of experiments, cortical sheets were perfused with aCSF containing 7.8mM Ca<sup>2+</sup> both in the presence and absence of EGTA in the recording electrode.

***Anoxic and Adenosine Experiments.*** In two separate sets of experiments, 5mM EGTA was removed from the recording electrode and cortical sheets were perfused with either anoxic aCSF or normoxic aCSF containing 200μM adenosine. Both sets of experiments were conducted to determine if anoxia and adenosine modulate G<sub>w</sub> through changes in intracellular Ca<sup>2+</sup>.

***A<sub>1</sub> Adenosine Receptor Experiments.*** To determine if G<sub>w</sub> modulation is adenosine receptor based recordings were obtained from cortical sheets perfused with 200μM adenosine. To distinguish between metabolic and receptor based effects tissue was perfused with either 1, 10, or 100μM N6-Cyclopentyladenosine (CPA), a selective A<sub>1</sub> adenosine receptor agonist. To further characterise the receptor based response cortical sheets were preincubated for 10 min with 1μM 8-Cyclopentyl-1,3-dipropylxanthine (DPCPX), an adenosine receptor blocker, and then perfused with 200μM adenosine and 1μM DPCPX, followed by a recovery perfusion. In a similar fashion anoxic experiments were performed on tissue preincubated and perfused with 1μM DPCPX.

***Tissue Viability and Energy Charge Determination.*** Tissue viability was assessed by measurement of [ATP], [ADP], and [AMP] and subsequent energy charge calculation (as described by Atkinson, 1977) in cortical sheets incubated for 0, 40, and 80min in aCSF containing 1.2, 4, and 7.8mM  $\text{Ca}^{2+}$ . For this purpose, individual cortical sheets were weighed and rapidly placed into 0.5ml of boiling 50mM HEPES buffer at pH 7.8 and sonicated for 25s. They were incubated at high temperature for an additional 3 minutes before being removed and chilled in an ice bath for 5min. The samples were then centrifuged for 10min at 10,000 RCF at 2°C and a 400µl aliquot of supernatant used for adenosine nucleotide determination by high performance liquid chromatography. To separate these nucleotides, a reverse phase column (150 x 4.6mm) (Supelco Model LC-18-T, Scarborough, ON, Canada) was used. For the mobile phase, 2 buffer solutions were used: Buffer A (0.1M potassium phosphate buffer/4mM tetrabutylammonium hydrogen sulfate (Sigma, ON, Canada) in deionized water, adjusted to pH 6.0 with KOH) and Buffer B (70% Buffer A: 30% Methanol). Buffer solutions were degassed with Helium prior to use. The gradient elution protocol consisted of an initial perfusion with 100% Buffer A, at 5min Buffer B gradient perfusion began, with the transition to 100% buffer B occurring at 13 min and lasting to 17 min. At this time the perfusion was switched back to Buffer A (100% at 18min) and perfused for an additional 7 min. Adenylate peaks were eluted at 1.5ml/min and a variable wavelength ultraviolet-visual spectrophotometer operating at 254nm was used for detection. The adenylate peak areas were quantified by comparison to known peak areas of ATP, ADP, and AMP standards.

## WHOLE CELL CAPACITANCE EXPERIMENTS

***Control and Anoxic Experiments.*** Experiments consisted of a 130 min time course where 2 control points ( $t=0,10$ ) were obtained before a 60min treatment perfusion. Control experiments involved brain sheets perfused for 130min with normoxic aCSF in the absence of EGTA in the recording electrode. For anoxic experiments the treatment reservoir was gassed with 95%N<sub>2</sub>/5%CO<sub>2</sub> and contained 0.5mM NaCN to prevent oxygenation artefacts, as described above.

***Calcium and Adenosine Experiments.*** To determine if high extracellular Ca<sup>2+</sup> levels could have an effect on C<sub>w</sub>, cortical sheets were perfused with normoxic aCSF containing 4mM Ca<sup>2+</sup>. In a separate set of experiments, cortical sheets were also perfused with aCSF containing 200μM adenosine to determine if high extracellular adenosine levels could effect C<sub>w</sub>. In both sets of experiments, EGTA was absent from the recording electrode and cortical slices were reperfused with normoxic aCSF after the treatment period to measure C<sub>w</sub> during the recovery 60min period.

***Lucifer yellow Experiments.*** To complement the normoxic and anoxic capacitance experiments the role of gap junctions was also visually examined. In two separate sets of experiments, turtle neurons were loaded with 1.2mM lucifer yellow (Sigma, ON, Canada) which was prepared in recording solution (as described in the Whole Cell Conductance and Capacitance measurements section). Lucifer yellow dye was present in the recording electrode and was introduced intracellularly when a whole cell configuration was achieved. Cortical sheets were then perfused with control and anoxic aCSF for a period of 30min. Dyed neurons were identified under oil immersion using a broad-spectrum fluorescent microscope (Olympus BH2) with an O-515 barrier filter to block out wavelengths less than 515nm.

## **STATISTICAL ANALYSIS**

Whole-cell conductance and capacitance data were analysed using a repeat measures analysis of variance (RM ANOVA) with a Dunnet's post hoc test to compare treatment values to control. The first 2 control time points (t=0, 10) were pooled together for comparison to the treatment values. The same statistical test using the control points individually does not alter the results. A similar test was used to detect differences amongst the energy charge values. All data are expressed as mean±SE.

## RESULTS

### WHOLE CELL CONDUCTANCE EXPERIMENTS

Under control conditions and using a standard electrode recording solution containing EGTA  $G_w$  was found to remain stable throughout a 130min time course (Fig. 11). Similarly, anoxic perfusion resulted in no significant changes in  $G_w$  (Fig 11). To test whether  $G_w$  is effected by elevated levels of  $Ca^{2+}$ ,  $Mg^{2+}$  and low pH, such as those measured in blood of dived turtles, tissue was perfused with a mimic aCSF solution under both normoxic and anoxic conditions (Fig.12). Following the initiation of normoxic or anoxic mimic aCSF perfusion a significant 31 and 26% reduction in  $G_w$  occurred,  $2.69\pm 0.26$  to  $1.86\pm 0.13nS$  at  $t=30$  ( $P=0.00869$ ) and  $2.61\pm 0.23$  to  $1.94\pm 0.19nS$  at  $t=30$  ( $P=0.00914$ ), respectively. In both sets of experiments  $G_w$  returned to control values within 20 min of control aCSF reperfusion. Exclusion of EGTA from the recording electrode during anoxic aCSF perfusion did result in a significant decrease in  $G_w$  ( $3.37\pm 0.34$  to  $2.46\pm 0.30nS$  at  $t=60$ ,  $P=0.0014$ ), subsequently returning to control values upon normoxic reperfusion (Fig. 13). The removal of EGTA from the recording electrode had no effect on the normoxic control values (Fig. 13).

Perfusion of cortical sheets with aCSF containing either low pH (7.1) or high  $Mg^{2+}$  (4.7mM) did not result in any significant changes in  $G_w$  (Fig. 14). To further investigate the role of calcium in modulating  $G_w$  perfusion of cortical sheets with control aCSF containing 4 and 7.8mM  $Ca^{2+}$  were carried out (Fig. 15). Perfusion with aCSF containing 4mM  $Ca^{2+}$ , without EGTA in the recording electrode, resulted in a significant 36% decrease in  $G_w$  ( $3.72\pm 0.22$  to  $2.40\pm 0.22nS$  at  $t=50$ ,  $P=0.0156$ ). Perfusion with aCSF containing 7.8mM  $Ca^{2+}$ , in the absence of EGTA, resulted in a 52% reduction in  $G_w$  ( $3.65\pm 0.59$  to  $1.78\pm 0.29nS$  at  $t=50$ ,  $P=0.0269$ ). In the absence of EGTA the whole cell configuration consistently broke



**Fig. 11.** The effect of anoxic perfusion on  $G_w$ . Control normoxic and anoxic perfusions with EGTA in the recording electrode. Horizontal bars indicate the treatment perfusion duration. All  $G_w$  data are the mean  $\pm$  SE, and comprise 6 to 9 separate experiments.

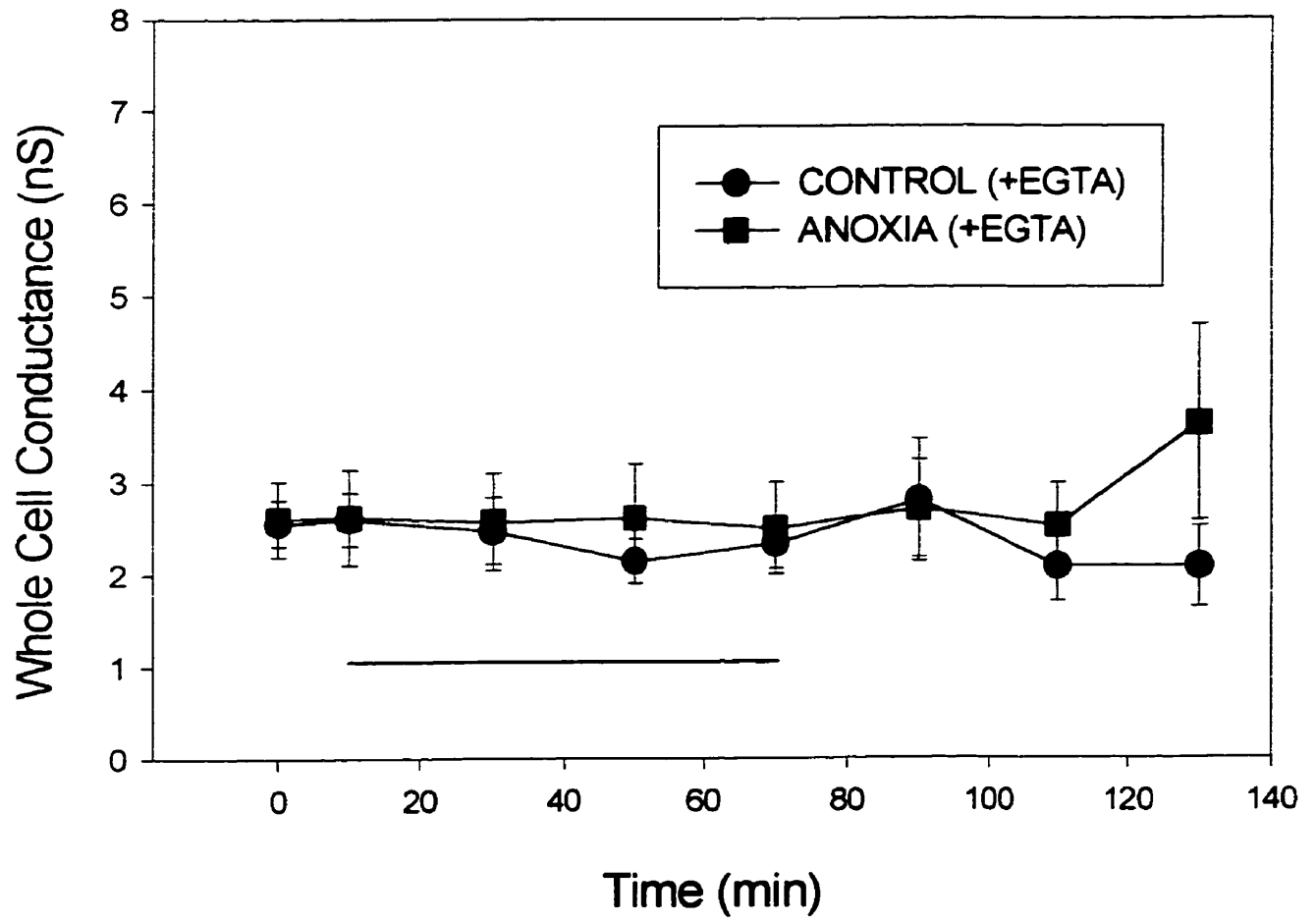


**Fig. 12.** The effect of mimic aCSF perfusion on  $G_w$ . Anoxic and normoxic mimic aCSF perfusions with EGTA in the recording electrode. Horizontal bars indicate the treatment perfusion duration. Asterisks indicate values that are significantly different from control values when analysed using a Dunnett's repeat measures ANOVA,  $P < 0.05$ . All  $G_w$  data are the mean  $\pm$  SE, and comprise 6 to 9 separate experiments.

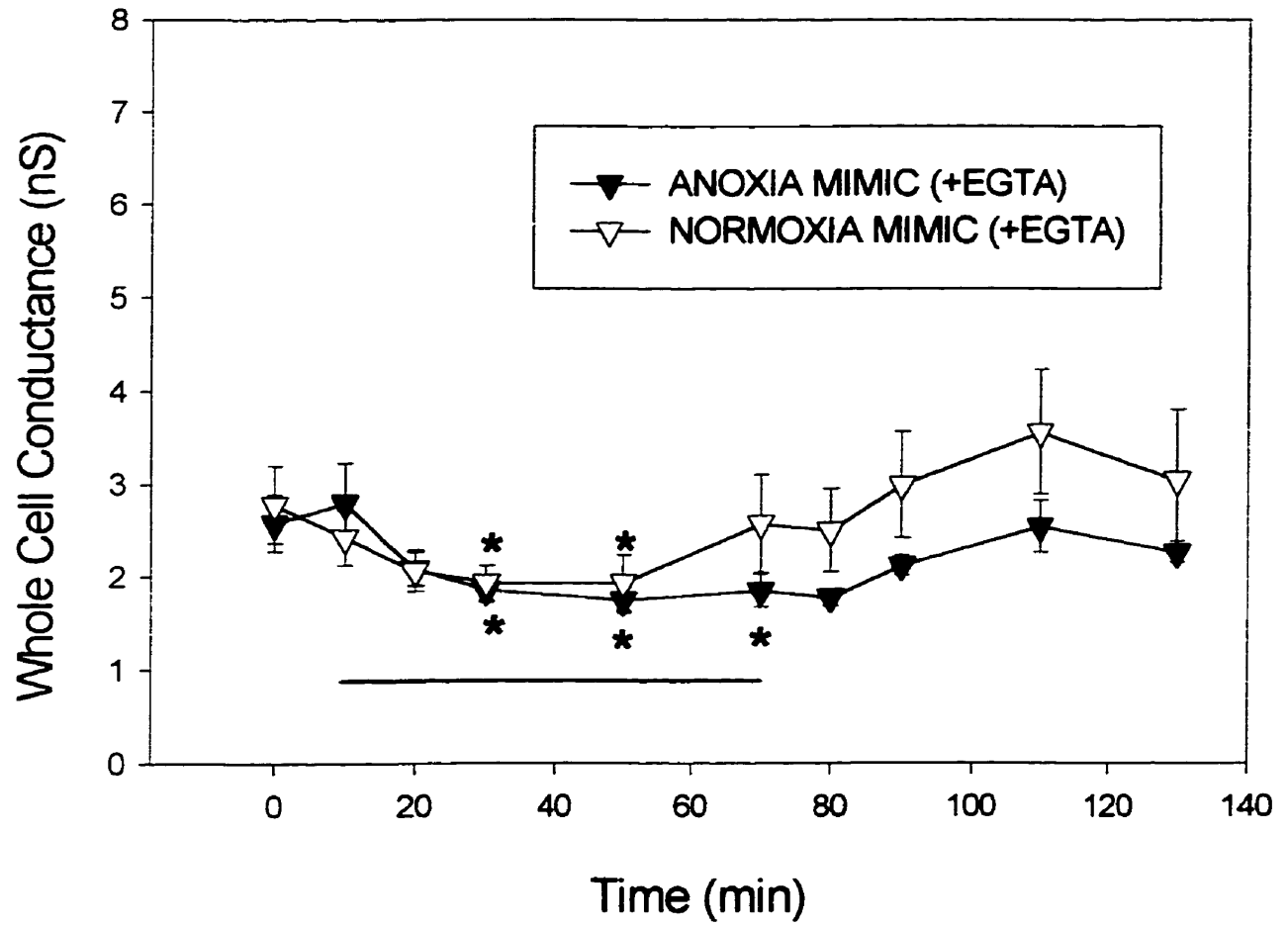


**Fig. 13.** The effect of anoxic perfusion on  $G_w$ . Control normoxic and anoxic perfusions without EGTA in the recording electrode. Horizontal bars indicate the treatment perfusion duration. Asterisks indicate values that are significantly different from control values when analysed using a Dunnett's repeat measures ANOVA,  $P < 0.05$ . All  $G_w$  data are the mean  $\pm$  SE, and comprise 6 to 9 separate experiments.

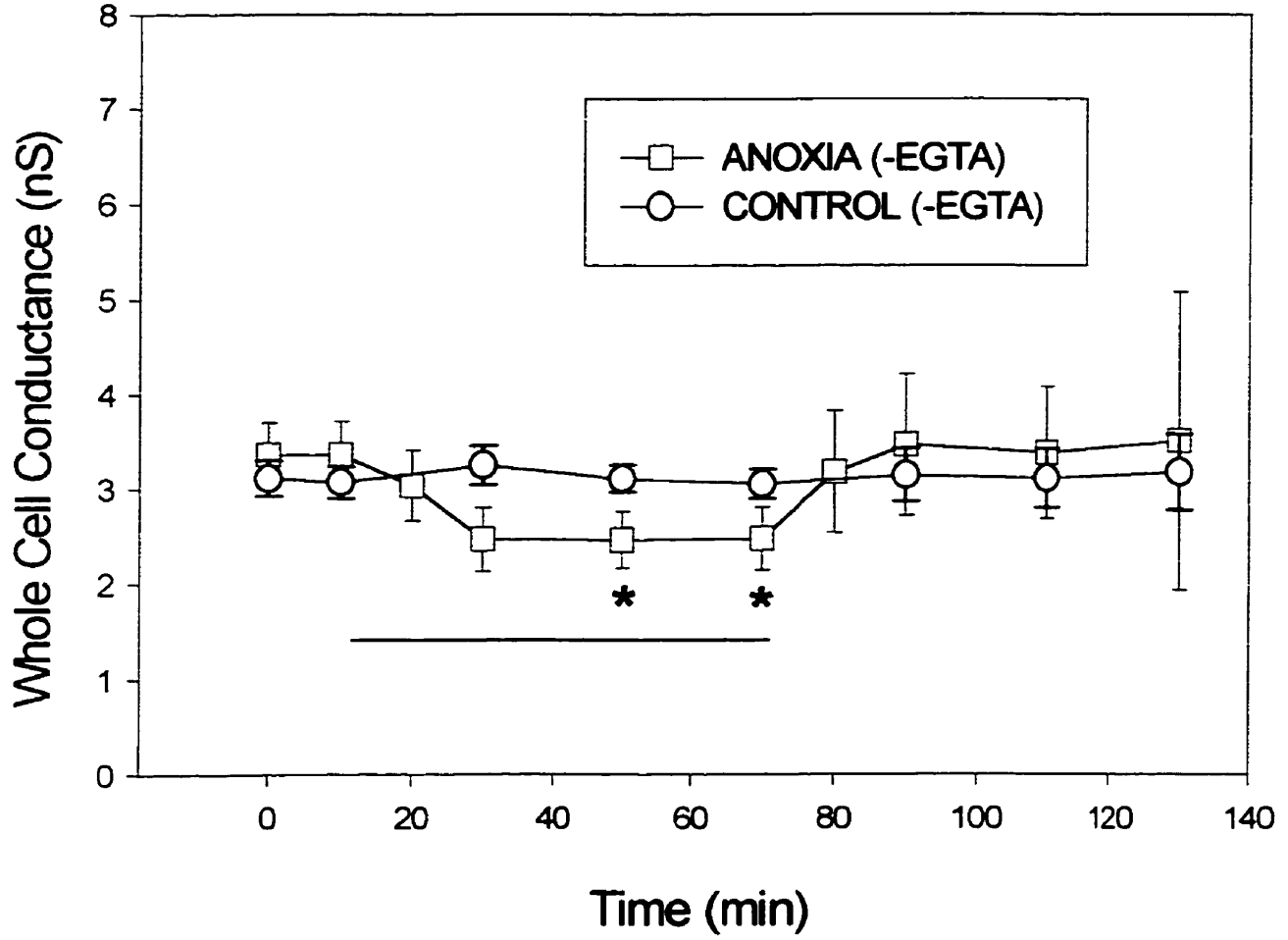
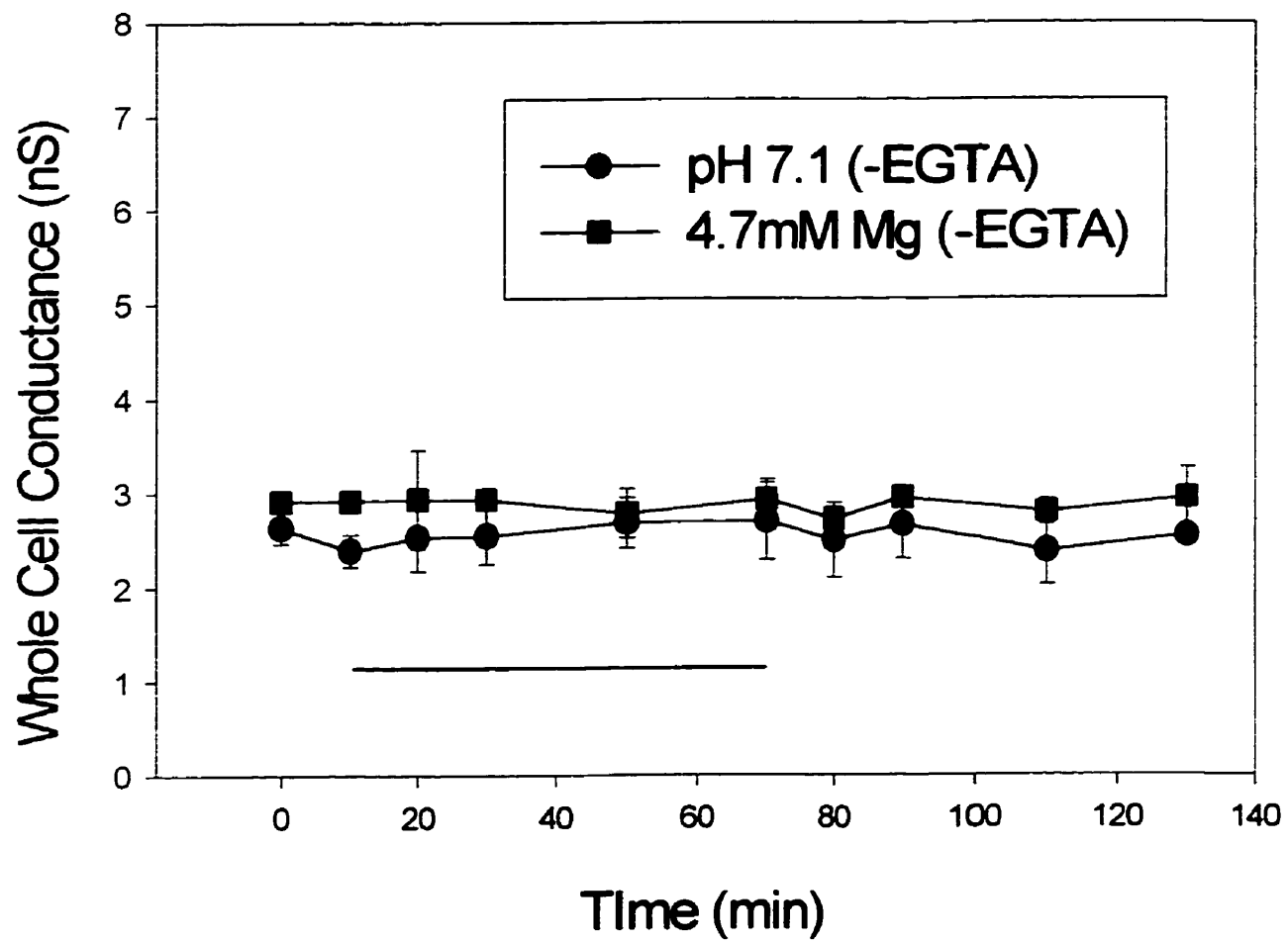


**Fig. 14.** The effect of low pH and high  $Mg^{2+}$  aCSF perfusion on  $G_w$ . Normoxic aCSF perfusions containing either low pH (7.1) or high  $Mg^{2+}$  (4.7mM) without EGTA in the recording electrode. Horizontal bars indicate the treatment perfusion duration. All  $G_w$  data are the mean  $\pm$  SE, and comprise 6 to 9 separate experiments.





down at  $t=50$ min. However, with inclusion of EGTA in the recording electrode the whole cell configuration was maintained throughout the treatment and recovery period, and a 32% reduction in  $G_w$  was measured with the 7.8mM  $Ca^{2+}$  treatment ( $2.68\pm 0.13$  to  $1.82\pm 0.16$ nS at  $t=50$ ,  $P=0.0000227$ ).

Tissue [ATP], [ADP] and [AMP] were determined from cortical sheets incubated for 0, 40 and 80min in saline containing 1.2mM, 4mM and 7.8mM  $Ca^{2+}$ . Energy charge values were calculated to determine if high  $[Ca^{2+}]_o$  was injurious to the cortical sheets resulting in loss of the whole-cell configuration. Tissue [ATP] and energy charge did not change significantly at any  $[Ca^{2+}]$  or exposure duration, values ranged from  $0.69\pm 0.06$  to  $0.72\pm 0.03$  and from  $1.91\pm 0.05$  to  $2.58\pm 0.24$   $\mu\text{mol. g wet weight}^{-1}$ , respectively (Table 1). Tissue [ADP] and [AMP] were typically  $0.81\pm 0.09$  and  $0.43\pm 0.03$   $\mu\text{mol. g wet weight}^{-1}$ , respectively.

The role of adenosine in modulating  $G_w$  was investigated similarly in the presence and absence of EGTA (Fig. 16). Perfusion with aCSF containing 200 $\mu\text{M}$  adenosine in the absence of EGTA resulted in a reduction in  $G_w$  from  $3.16\pm 0.17$  to  $2.17\pm 0.34$ nS at  $t=50$  ( $P=0.00916$ ), with  $G_w$  returning to control values within 30min of reperfusion with control aCSF. The inclusion of EGTA in the recording electrode blocked any changes in  $G_w$ . To determine if the adenosine effect was receptor specific cortical sheets were perfused with varying concentrations of CPA (0.1, 10, 100 $\mu\text{M}$ ) (Fig. 17). Although 0.1 $\mu\text{M}$  and 10 $\mu\text{M}$  CPA perfusion of the cortical tissue resulted in modest decreases in  $G_w$  these effects were not statistically significant. However, 100 $\mu\text{M}$  CPA treatment resulted in a significant reduction in  $G_w$  ( $3.25\pm 0.25$  to  $2.41\pm 0.34$ nS at  $t=20$ ,  $P=0.00361$ ).

To further characterise the role of adenosine in  $G_w$  regulation, adenosine and anoxic perfusion experiments were carried out in the presence of the  $A_1$  receptor specific antagonist

**Fig. 15.** Whole cell conductance measurements obtained during perfusion with control aCSF containing either 4mM and 7.8mM  $\text{Ca}^{2+}$  with and without EGTA in the recording electrode. Horizontal bar indicates the treatment perfusion duration. Asterisks indicate values that are significantly different from control values when analysed using a Dunnett's repeat measures ANOVA,  $P < 0.05$ . All  $G_w$  data are the mean  $\pm$  SE, and comprise 6 to 9 separate experiments.

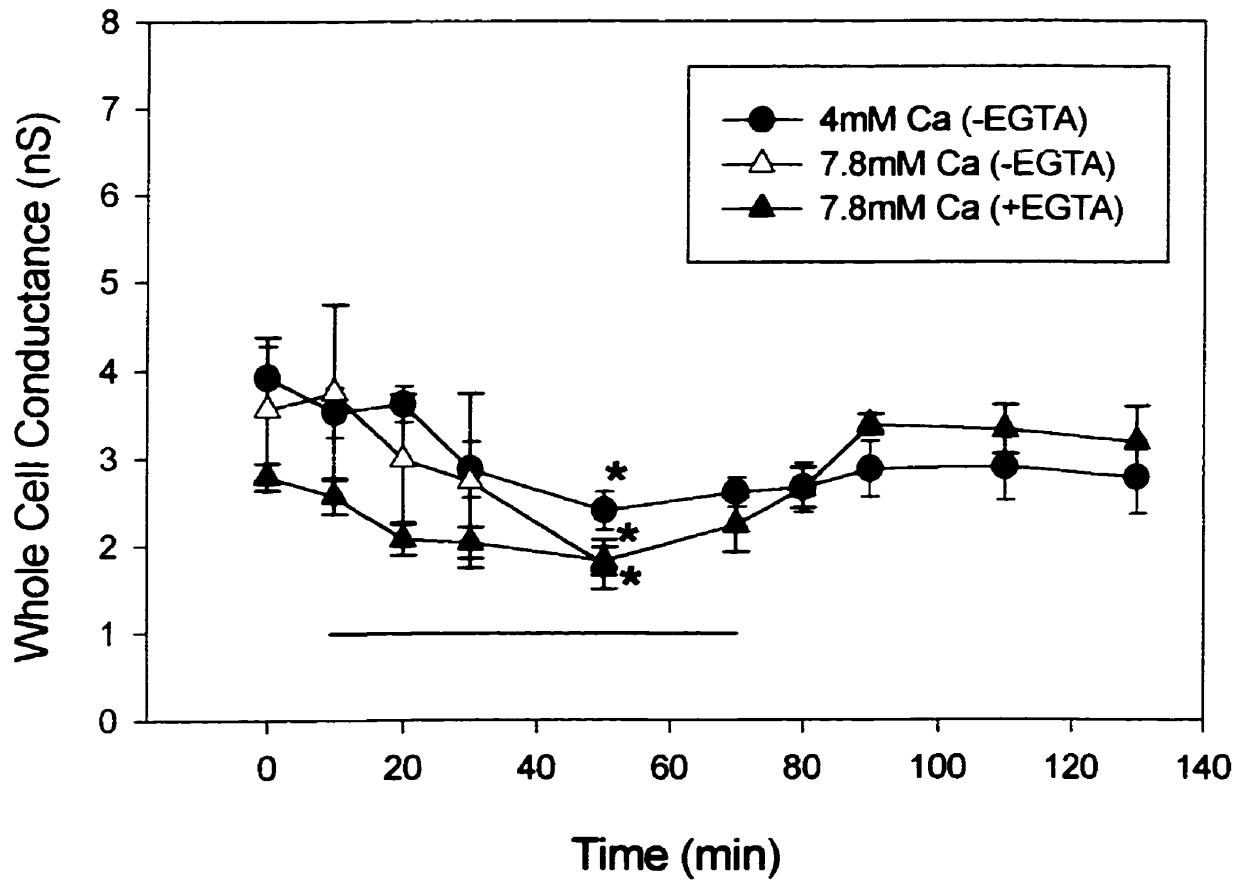
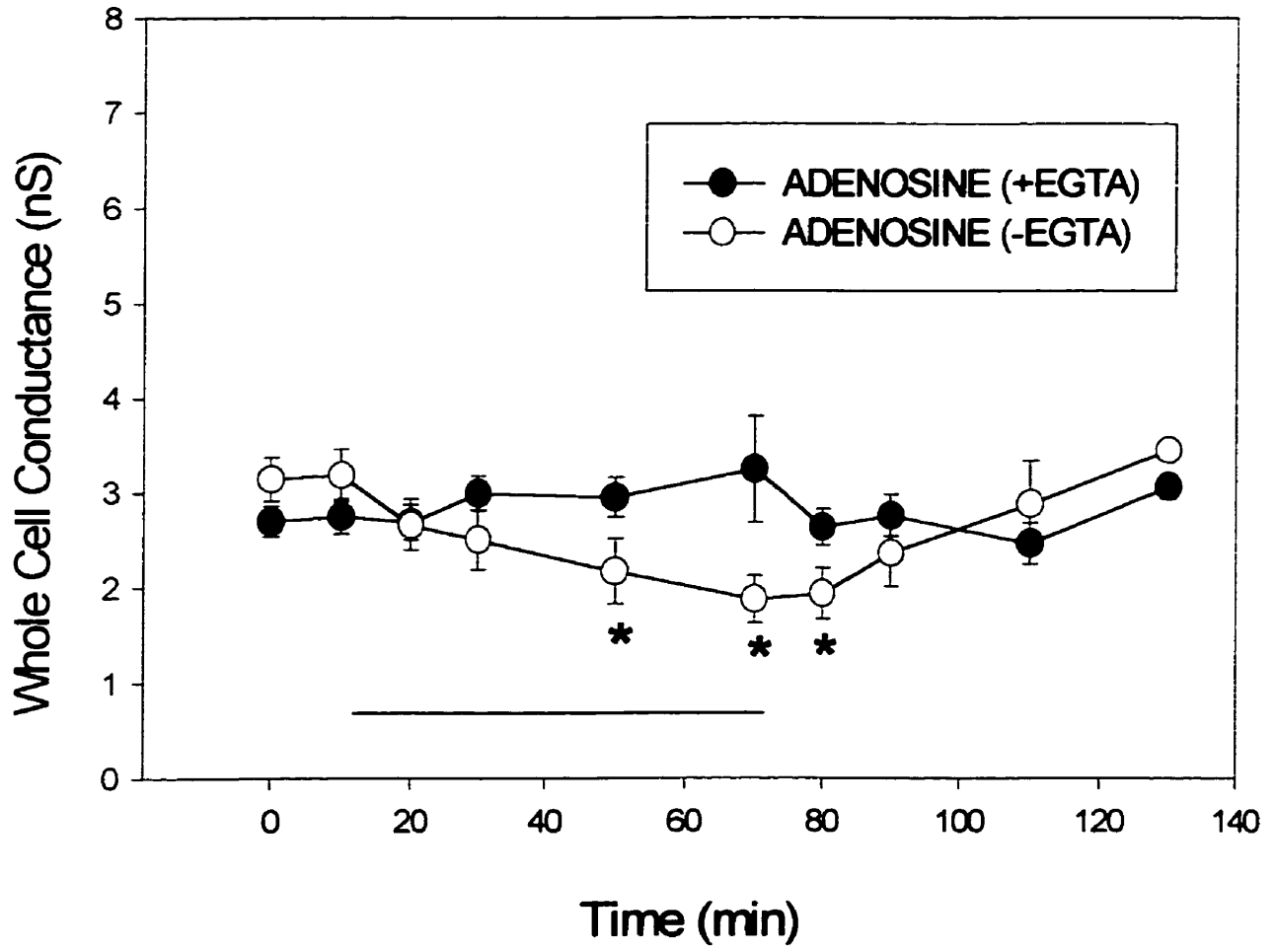


Table 1. Cortical sheet energy charge and [ATP] upon exposure to varying  $[Ca^{2+}]$

		TIME (min)		
		0	40	80
1.2mM $Ca^{2+}$ (Control)	EC	0.71±0.04	0.70±0.04	0.69±0.06
	[ATP]*	1.91±0.05	1.98±0.37	1.95±0.24
4mM $Ca^{2+}$	EC		0.71±0.07	0.70±0.06
	[ATP]		2.58±0.22	2.09±0.15
7.8mM $Ca^{2+}$	EC		0.70±0.04	0.72±0.03
	[ATP]		2.58±0.24	1.92±0.25

[ATP]\* in  $\mu\text{mol. g wet weight}^{-1}$ . Energy charge (EC) values were calculated using the formula  $EC = \frac{ATP + 0.5(ADP)}{ATP + ADP + AMP}$ . Values are mean  $\pm$  SE, and comprise 6 to 8 separate experiments.

**Fig. 16.** Whole cell conductance measurements obtained during a 200 $\mu$ M adenosine perfusion (duration indicated by bar) with and without EGTA in the recording electrode. Asterisks indicate values that are significantly different from control values when analysed using a Dunnett's repeat measures ANOVA,  $P < 0.05$ . All  $G_w$  data are the mean  $\pm$  SE, and comprise 7 to 9 separate experiments.



**Fig. 17.** Acute tissue perfusion with solutions containing varying CPA concentrations in the absence of EGTA. Horizontal bar indicates the treatment perfusion duration. Asterisks refer to the 100 $\mu$ M CPA experiment only and indicate values that are significantly different from control values when analysed using a Dunnett's repeat measures ANOVA,  $P < 0.05$ . All  $G_w$  data are the mean  $\pm$  SE, and comprise 6 to 8 separate experiments.

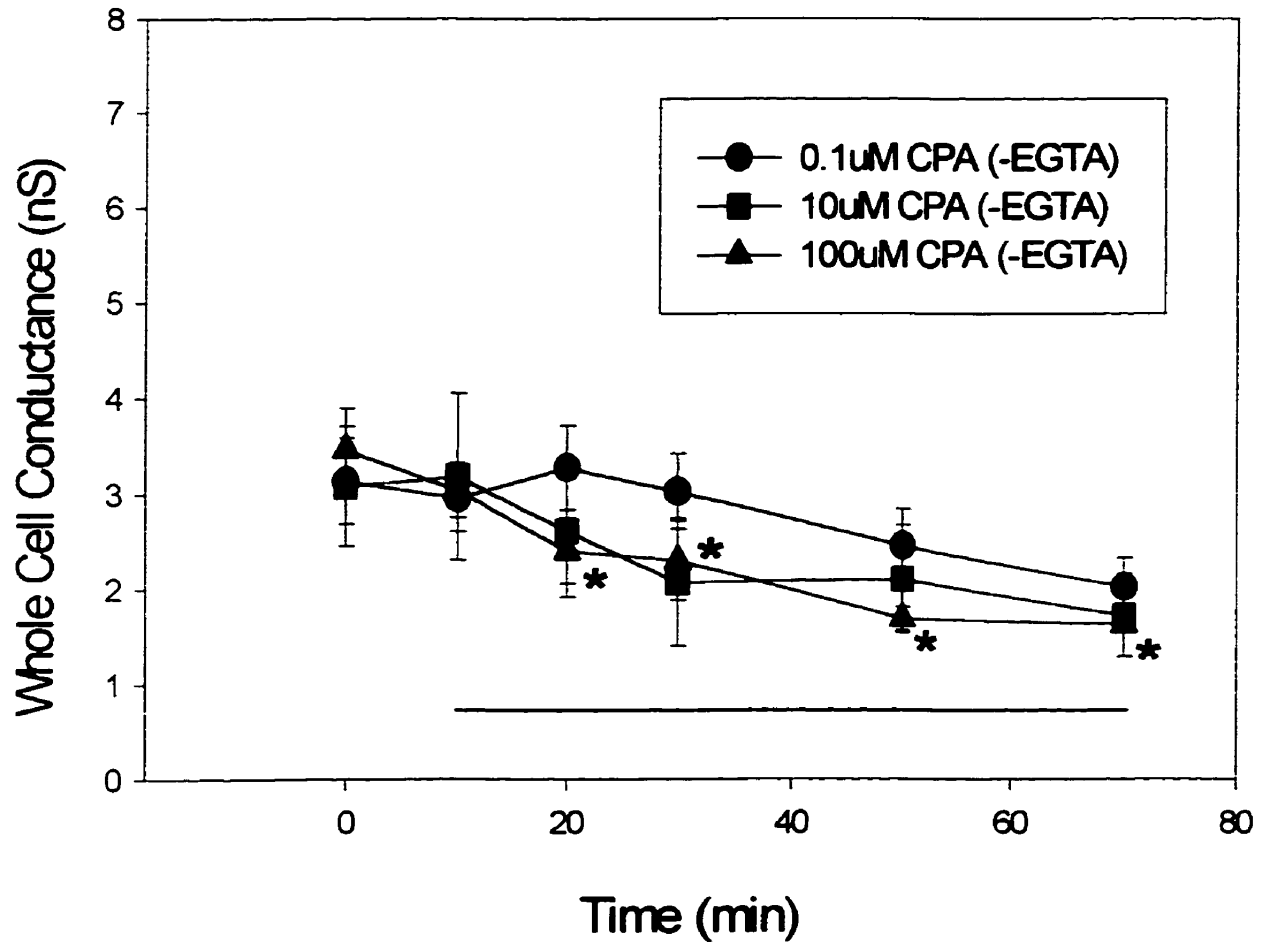
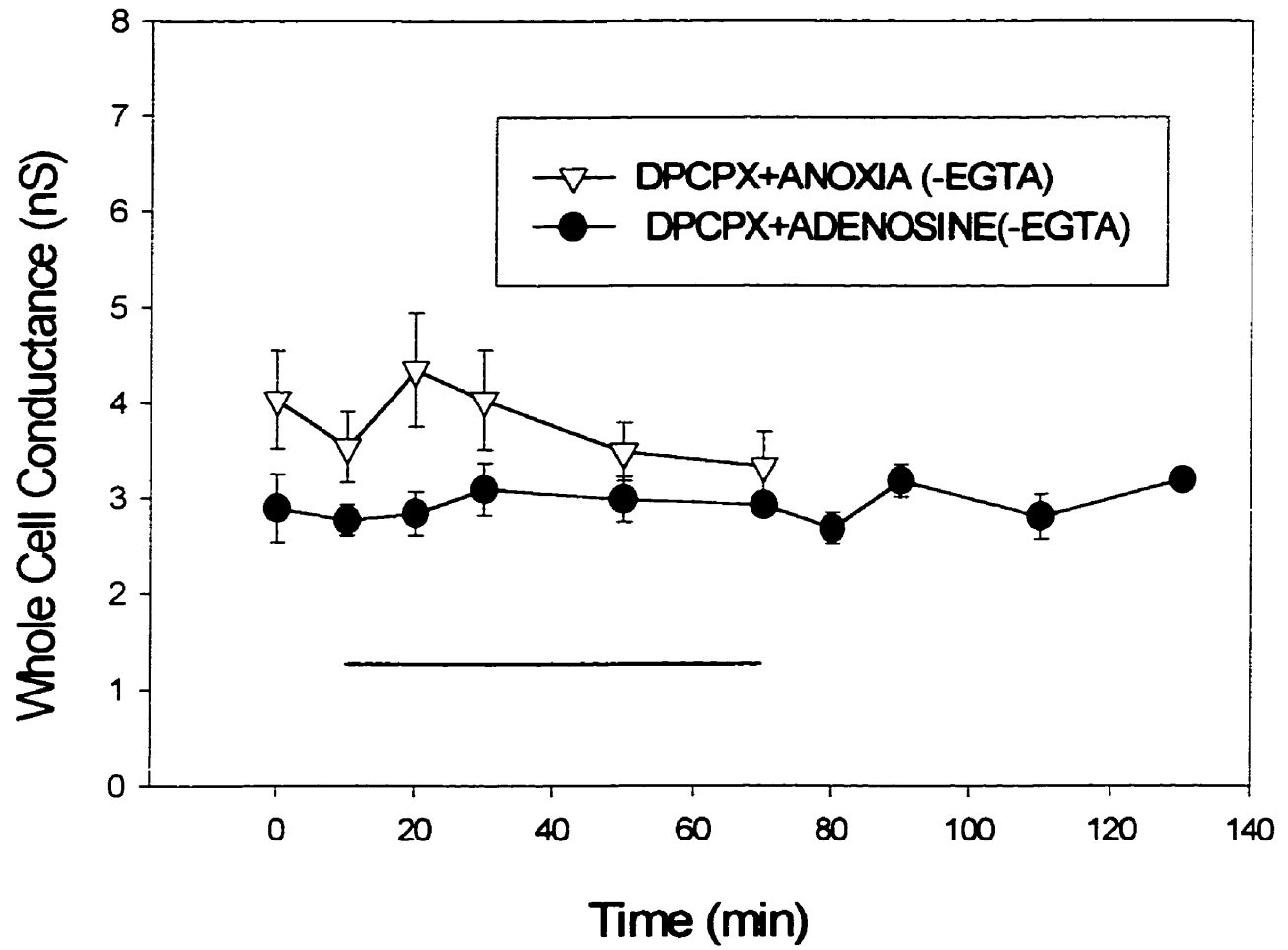




**Fig. 18.** The effect of the A<sub>1</sub> receptor antagonist DPCPX on G<sub>w</sub> during anoxic and adenosine perfusions (duration indicated by horizontal bar). All G<sub>w</sub> data are the mean ± SE, and comprise 6 to 8 separate experiments.



DPCPX (Fig. 18). Under these conditions neither adenosine nor anoxia had significant effects on  $G_w$ . To rule out artefacts resulting from DPCPX alone cortical slices were perfused with 0.1 $\mu$ M DPCPX for 50min with no significant reductions in  $G_w$  (data not shown).

### WHOLE CELL CAPACITANCE EXPERIMENTS

Under control conditions and using an EGTA-free electrode recording solution  $C_w$  was found to remain stable throughout a 130min time course (Fig. 19). Similarly, anoxic perfusion resulted in no significant changes in  $C_w$ , capacitance values ranged from  $45.5 \pm 5.7$  to  $60.1 \pm 6.2$  pF (Fig. 19). To further investigate the role of calcium in modulating  $C_w$  perfusion of cortical sheets with control aCSF containing 4mM  $Ca^{2+}$  were carried out. In the absence of EGTA from the recording electrode, the 4mM  $Ca^{2+}$  perfusion also did not result in a significant decrease in  $C_w$  (Fig. 20). Additionally, capacitance values were unaffected by adenosine perfusion and did not change significantly from control values (Fig. 20). To visually inspect whether gap junction permeability changes in turtle brain, neurons were loaded with 1.2mM Lucifer yellow which was present in the recording electrode. Cortical sheet neurons did not show dye propagation to neighbouring cells during either a normoxic (Fig. 21A) or anoxic perfusion (Fig. 21B).

**Fig. 19.** The effect of anoxic perfusion on  $C_w$ . Control normoxic and anoxic perfusions without EGTA in the recording electrode. Horizontal bars indicate the treatment perfusion duration. All  $G_w$  data are the mean  $\pm$  SE, and comprise 6 to 9 separate experiments.

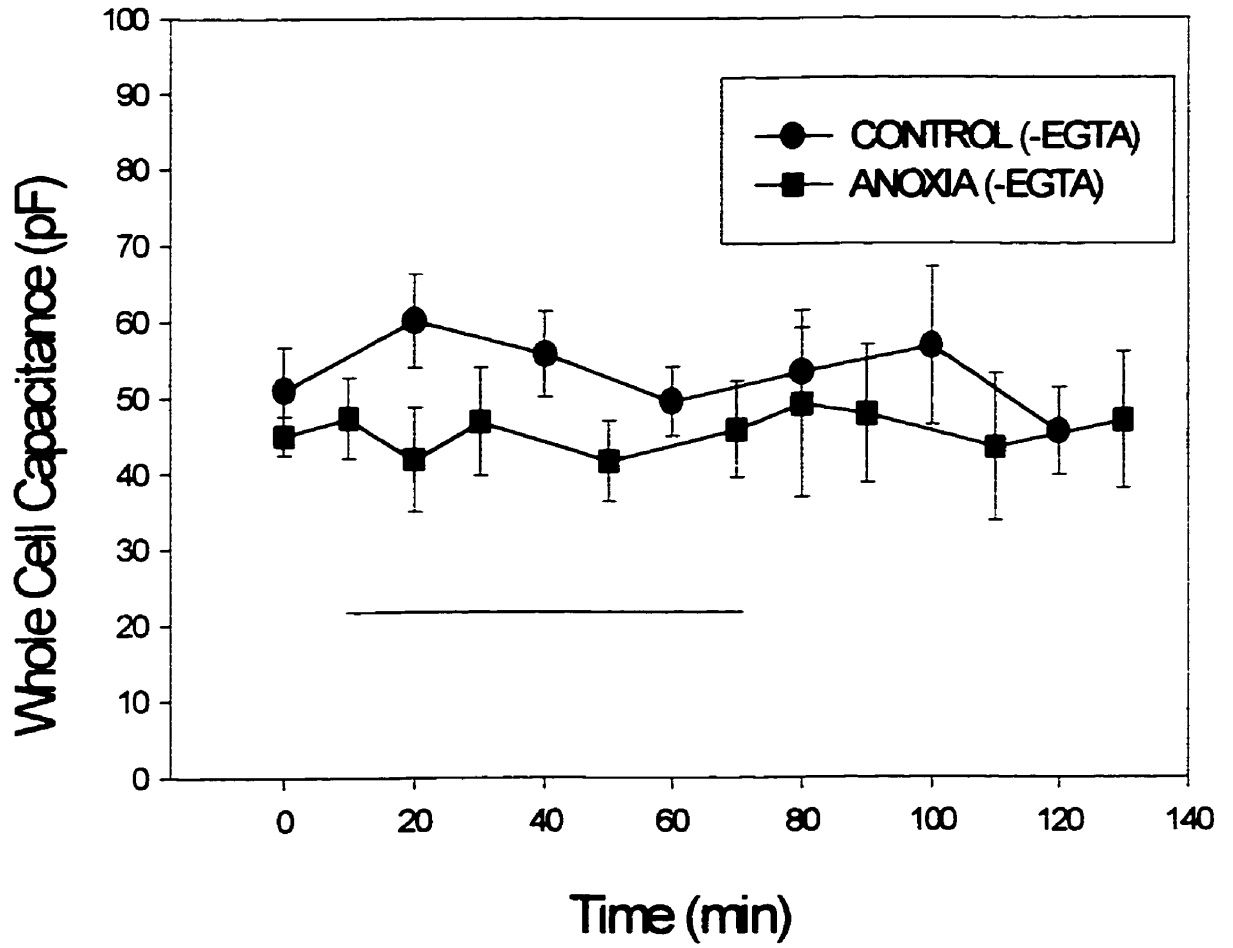


**Fig. 20.** Whole cell capacitance measurements obtained during perfusion with control aCSF containing either 200 $\mu$ M Adenosine or 4.0mM Ca<sup>2+</sup> without EGTA in the recording electrode. Horizontal bar indicates the treatment perfusion duration. All G<sub>w</sub> data are the mean  $\pm$  SE, and comprise 8 to 10 separate experiments.

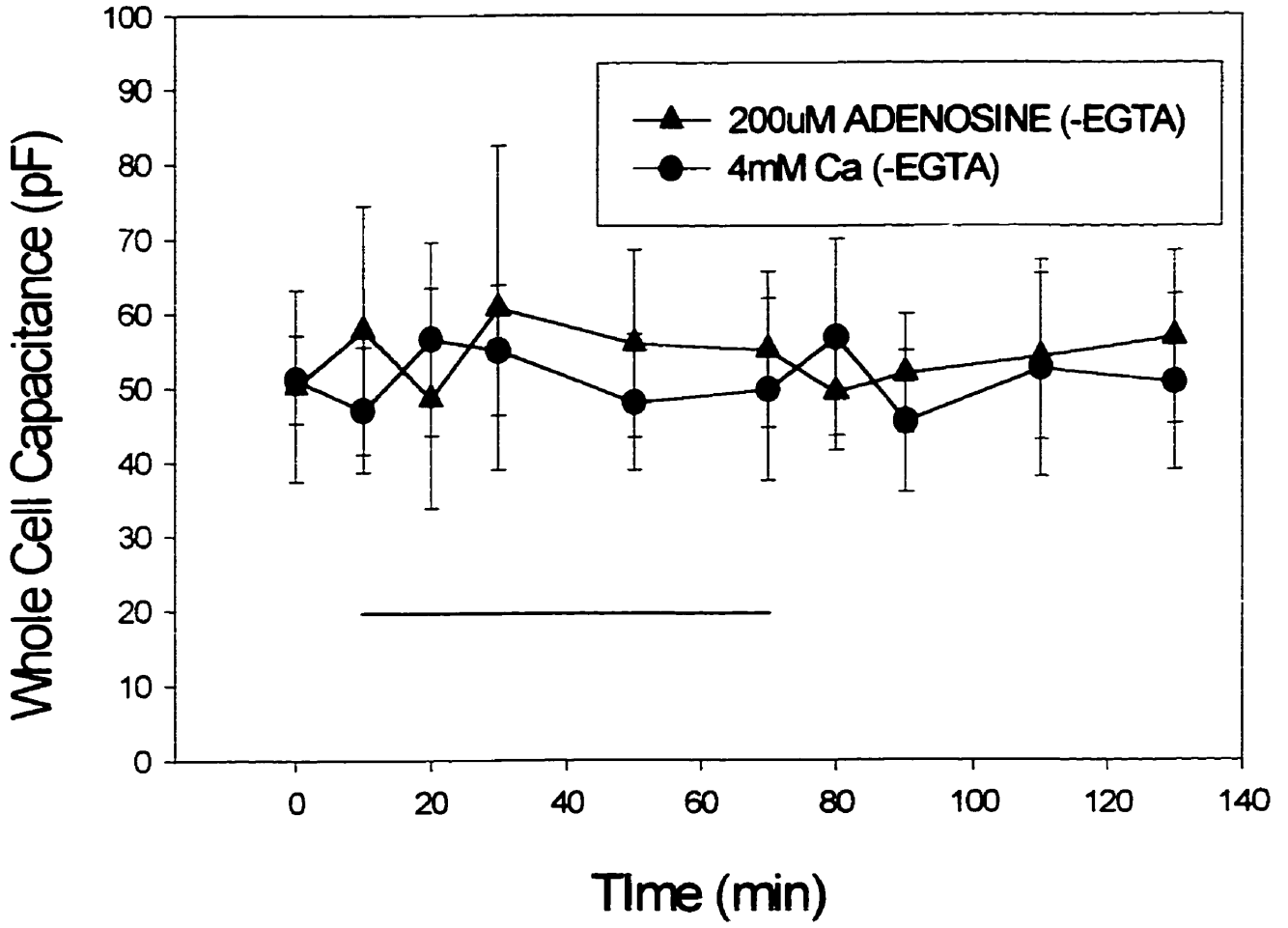
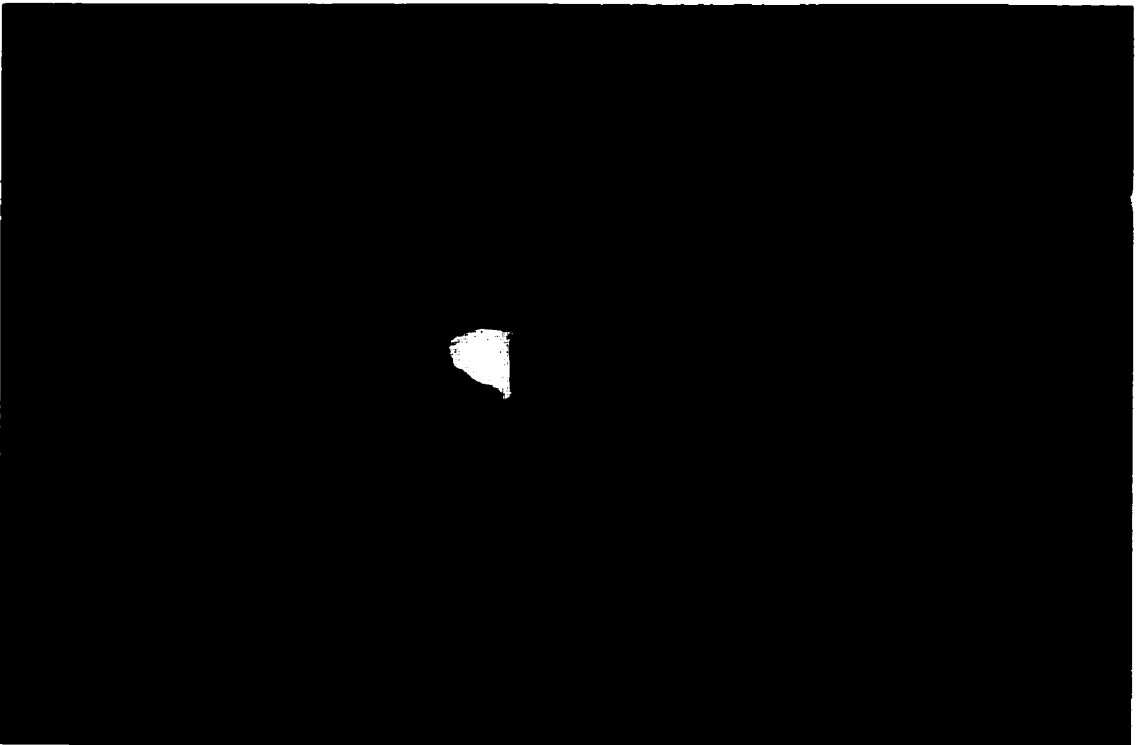
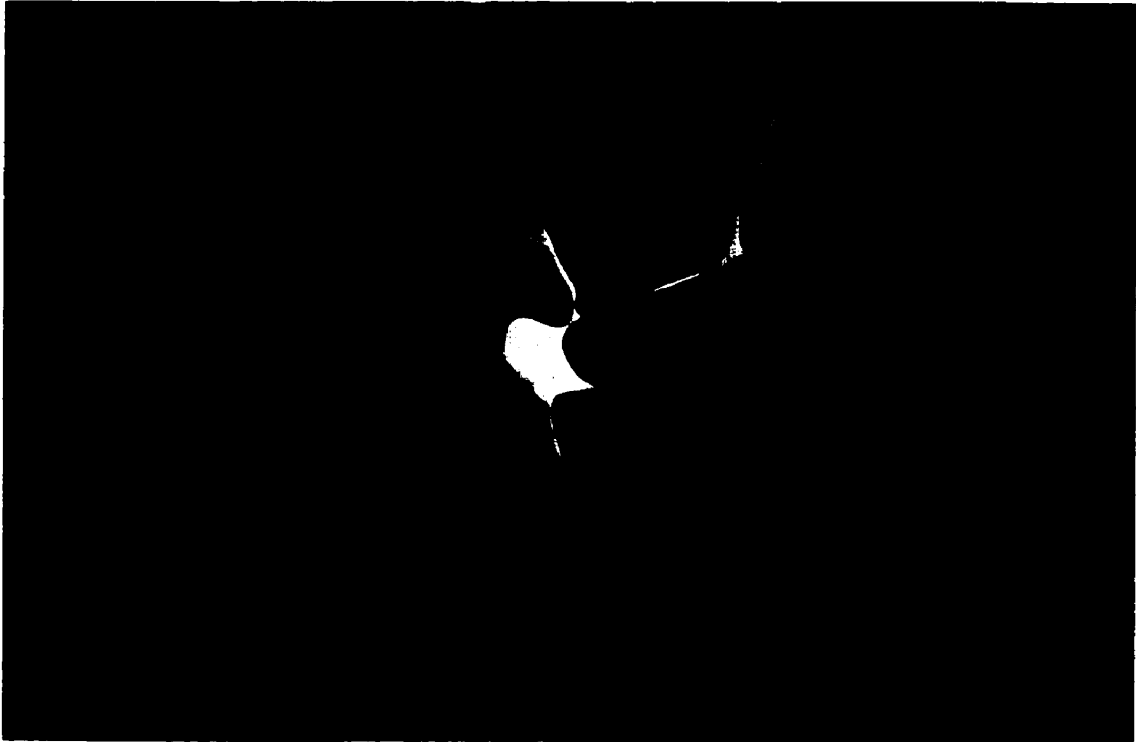


**Fig 21.** Lucifer-yellow loaded neurons (1.2mM) using patch clamp electrodes under (A) normoxic and (B) anoxic perfusion during a 30min treatment. Both images are representative of 6 experiments each. Scale; A: 1cm=24.5 $\mu$ m, B: 1cm=17.9 $\mu$ m.





## DISCUSSION

The results show that whole cell conductance decreases in anoxic turtle brain. This finding is in contradiction to that previously reported by Doll et. al. (1991) where no change in neuronal  $G_w$  was detected during anoxic perfusion. It is unlikely that the relatively high resistance (30-70M $\Omega$ ) electrodes used in the previous study compromised measurement of  $G_w$ , since their values for  $G_w$  ( $2.73\pm 0.36$ nS; Doll et. al., 1991) are similar to our values ( $2.80\pm 0.30$ nS) and those reported in mammalian brain ( $5.68\pm 0.60$ nS; Seutin et. al., 1996). Rather it is likely that the inclusion of EGTA (10mM) in their recording electrode that prevented an anoxia-induced decrease in  $G_w$ , since the inclusion of EGTA in the recording electrode of this study also prevented changes in  $G_w$ . Additionally, the findings support the second prediction of the “channel arrest” hypothesis that anoxia tolerant species ought to have mechanisms to acutely regulate cellular ion permeability.

Both a normoxic and anoxic mimic perfusion significantly decreased  $G_w$ , indicating that either elevated levels of  $Ca^{2+}$ ,  $Mg^{2+}$ , or low pH or a combination of these constituents is responsible for the observed reduction in  $G_w$ . Perfusion of cortical sheets with aCSF containing high  $Mg^{2+}$  or low pH (7.1) did not alter  $G_w$  significantly. However, increasing the perfusate  $[Ca^{2+}]$  from 1.2 to 4 and 7.8mM did result in significant reductions in  $G_w$ . Since  $[Ca^{2+}]_o$  increases in turtle blood throughout an anoxic dive (Herbert and Jackson, 1985a) and it has been recently shown that neuronal  $[Ca^{2+}]_i$  increases in anoxically dived turtles (Bickler, 1998), then it is possible that increases in  $[Ca^{2+}]_o$  may result in changes in  $[Ca^{2+}]_i$ . This may be an important event leading to decreased membrane ion permeability and therefore  $G_w$ .

Adenosine perfusion also reduced  $G_w$  suggesting a role for adenosine in channel arrest. This response is likely receptor mediated since the  $A_1$  specific receptor agonist CPA

decreased  $G_w$  in a concentration dependent manner. Moreover, the potent  $A_1$  receptor antagonist DPCPX blocked the adenosine mediated decrease in  $G_w$ , further strengthening the argument for a receptor based mechanism. The antagonist also prevented the anoxia induced reductions in  $G_w$  suggesting that endogenous adenosine released from cortical sheets during anoxia results in the observed decrease in  $G_w$ .

All cells leak ions at rest. Leakage is defined as the movement of an ion species down its electrochemical gradient. Earlier voltage-clamp studies conducted by Hodgekin and Huxley (1952) were the first to recognize a voltage-independent background conductance, dubbed “leakage conductance”, of undetermined ionic basis. Although this leakage conductance is thought to be voltage-independent and important in setting the resting potential of the neuron, very little information has become available to further identify which ions are responsible for this background conductance. Since neuronal  $Ca^{2+}$  and  $Na^+$  channels are predominantly voltage-sensitive and the resting leakage of  $Ca^{2+}$  and  $Na^+$  is relatively small, it is unlikely that these ions contribute significantly to the observed leakage conductance. Rather, the background conductance has been conventionally ascribed to the flux of  $K^+$  ions, reflecting an exceptionally high concentration of open voltage-insensitive  $K^+$  channels in the resting neuron (Hille, 1992).

The anoxia-induced reduction in  $G_w$  that was detected may involve the regulation of voltage-independent  $K^+$  channels, or “leakage  $K^+$  channels”. These channels are thought to contribute to basal leakage currents and may be involved in establishing a resting neuronal membrane potential. The tandem-pore domain outwardly rectifying  $K^+$  channel (TOK1), from the budding yeast *Saccharomyces cerevisiae*, was the first channel of this type to be cloned (Ketchum et. al., 1995). Several types of leakage  $K^+$  channels have been identified in

mammalian CNS, including the tandem-pore domain weak inward rectifier  $K^+$  channel (TWIK-1) (Lesage et. al., 1997) and the tandem-pore domain outward rectifier TREK-1 (Fink et. al., 1996). TWIK-1 is highly expressed in hippocampus and cerebral cortex and shares 28% homology with TREK-1 that is also found in the hippocampus, cerebral cortex and cerebellum (Fink et. al., 1996; Lesage et. al., 1997). More recently, the TWIK-related acid sensitive  $K^+$  channel (rTASK) has been demonstrated to be noninactivating at all membrane potentials tested, a manner which is characteristic of a background or leakage channel (Lesage, 1997).

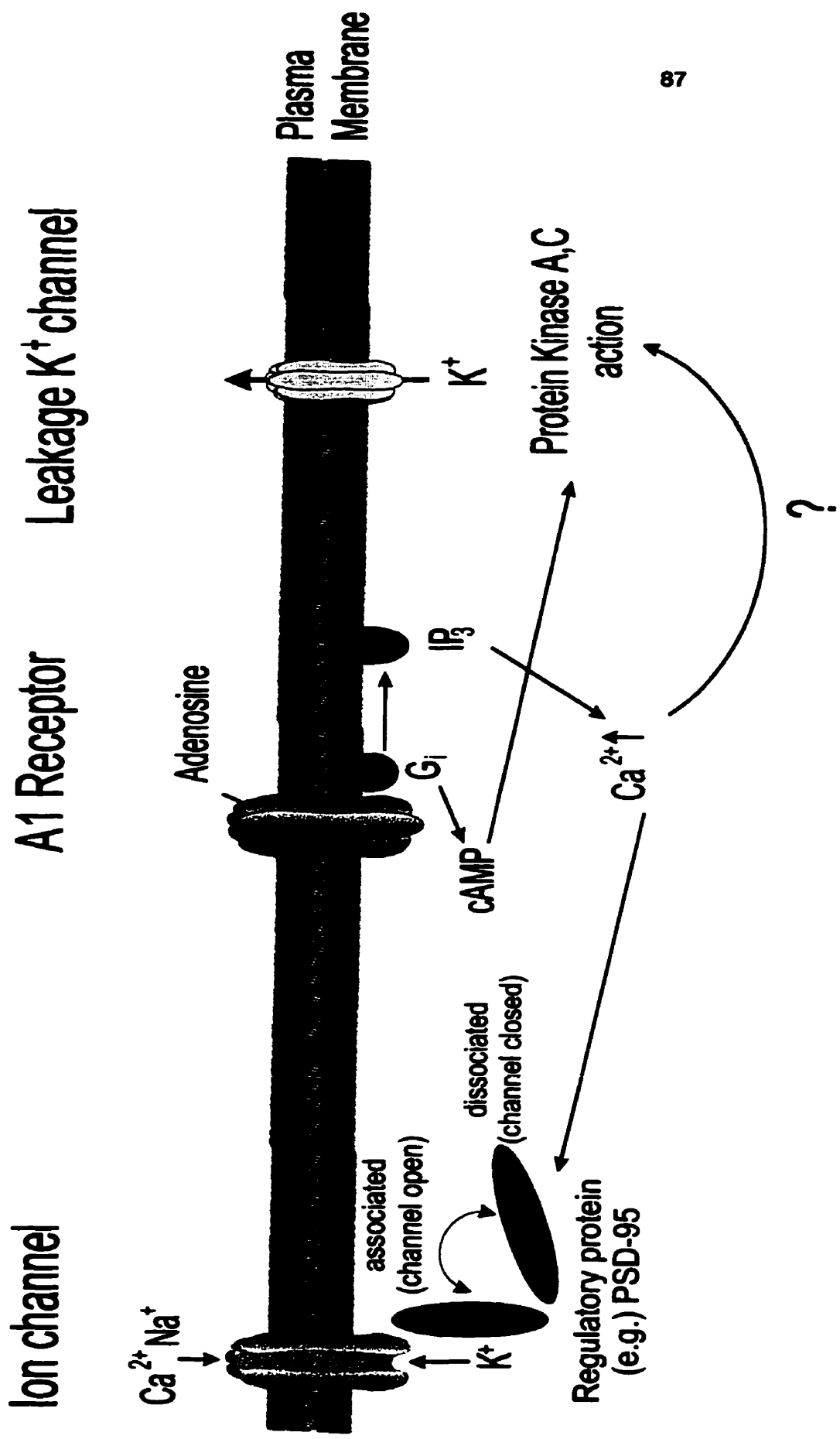
Intracellular protein kinases seem to produce important, differential modulation of these leakage  $K^+$  channels. Activators of protein kinase C potentiate TWIK-1 currents whereas TREK-1 currents are inhibited (Lesage et. al., 1996*a,b*). Furthermore, agents that increase intracellular cAMP levels and thereby activate protein kinase A significantly inhibit TREK-1 currents but have no effect on TWIK-1 currents (Fink et. al., 1996; Lesage et. al., 1996*b*). Similarly, the rTASK channel has been shown to have several regulatory sites, including protein kinases A,C, and tyrosine kinase and post synaptic density (PSD-95) sites (Leonoudakis et. al., 1998). Application of Forskolin (adenylate cyclase stimulator) to rTASK channels exogenously expressed in *Xenopus* oocytes results in a 42% reduction in  $K^+$  currents, suggesting that PKA can reduce rTASK channel permeability (Leonoudakis et. al., 1998). Recently, Buckler (1997) has shown that anoxia induces a significant reduction in the resting membrane conductance of rat carotid body type I cells through the inhibition of a background  $K^+$  conductance. Thus, it is possible that during the transition to anoxia  $K^+$  leakage channel permeability is decreased through the action of second messenger pathways, resulting in decreased  $G_w$  (Fig. 23).

Adenosine may play an important role in regulating  $K^+$  leakage channels. Failure of adenosine perfusion to illicit a reduction in  $G_w$  in the presence of EGTA suggests that adenosine exerts its effects through changes in  $[Ca^{2+}]_i$ . The  $A_1$  receptor is a G-protein linked receptor able to modulate several intracellular cascades including the phospholipase C (PLC)/inositol triphosphate ( $IP_3$ ) and adenylyl cyclase pathways (Rudolphi et. al., 1992). It is possible that during anoxia,  $A_1$  receptor activation leads to adenylyl cyclase activation via the G-protein pathway resulting in increased intracellular cAMP levels. Activation of protein kinase A due to changes in cAMP could result in the differential phosphorylation of various ion channels resulting in a down-regulation of their activity, thus reducing cellular ion permeability. Alternatively,  $A_1$  receptor activation could result in the production of  $IP_3$  via PLC which would result in increased intracellular  $Ca^{2+}$  levels. The anoxia-induced increase in intracellular calcium may function as a molecular switch as described for the neuronal  $Ca^{2+}$  binding protein Calmodulin, which regulates the action of various protein kinases and phosphatases (Ikura, 1996). These in turn change the phosphorylation state and thus permeability of ion channels and receptors resulting in an altered  $G_w$  (Fig. 23). How the intracellular second messenger traffic is regulated in a way that selectively regulates the activity of the appropriate protein kinases and phosphatases is uncertain.

An alternate target for calcium are proteins associated with the neuronal cytoskeleton that recognize and bind to specific C-terminus sequences of membrane proteins. These regulatory proteins are essentially an extension of the neuronal cytoskeleton (Gulley and Reese, 1981) and are thought to be important in the clustering and localization of a wide variety of voltage-dependent ion channels and ion transporters. Examples of these intracellular proteins include the post-synaptic density (PSD-95) family,  $\alpha$ -actinin and the

glutamate receptor interacting protein (GRIP) family which interact with and localize  $K^+$  channels, NMDA channels and glutamate receptors (Sheng and Wyszynski, 1997). Recently, Sattler et. al., (1999) have demonstrated that suppressing the PSD-95 protein in cultured cortical neurons blocked  $Ca^{2+}$  mediated toxicity as a result of NMDA receptor activation. Additionally, a reduction in NMDA channel activity has been demonstrated in response to increases in cytosolic calcium (Rosenmund and Westbrook, 1993). This suggests that cytoskeletal interactions are able to regulate the functions of NMDA channels in a calcium dependent manner. It has been postulated that NMDA channels are bound to a hypothetical regulatory protein, similar to those mentioned above, which normally functions to keep the channels open (Rosenmund and Westbrook, 1993). The NMDA channels inactivate when calcium increases intracellularly, binding to this hypothetical regulatory protein, dissociating it from the NMDA channel. Thus, it is possible that an  $A_1$  receptor mediated increase in cytosolic calcium may act to reduce the activity of leakage  $K^+$  channels and other channel types associated with the neuronal cytoskeleton in a similar fashion (Fig. 23), thereby inducing a macroscopic reduction in cell membrane permeability in the anoxic turtle brain.

**Fig. 22.** Summary of postulated mechanisms and sites for regulation of cell membrane permeability involved in conferring anoxia tolerance in the turtle brain.





Gap junctions represent well-documented means of intercellular communication in various tissues including the brain where they function to provide intercellular continuity among cells, facilitating the exchange of electrolytes, second messengers and metabolites between cells (Dermietzel and Spray, 1993). Since gap junction channels provided electrical continuity among cells, the functional importance of gap junction channels arises from their permeability and whether their opening and closing contributes to the changes in whole cell conductance mentioned above.

The results demonstrate that whole cell capacitance does not significantly change in the anoxic turtle brain. Furthermore, elevated levels of extracellular calcium (4mM) or adenosine (200 $\mu$ M) do not significantly affect gap junction permeability as corroborated by the lack of change in cortical sheet whole cell capacitance during these conditions. Finally, Lucifer Yellow introduced into turtle neurons did not diffuse to neighbouring cells during either normoxic or anoxic perfusion. One may conclude from the results that the observed changes in whole cell conductance cannot be attributed to any appreciable changes in gap junction permeability. To my knowledge, this study is the first to document the relevance of gap junctional coupling in the anoxic turtle neurons.

Although little or no evidence exists to shed light on the physiological role gap junctions serve in the turtle brain, several studies convincingly demonstrate that gap junctional coupling is subject to high plasticity in the turtle retina, and is regulated by functional factors including neurotransmitter action (Firsov and Green, 1998; Janssen-Bienhold et. al., 1998; Ammermuller et. al., 1996). Gap junctions provide electrical coupling among horizontal cells in turtle retinae and have been shown to close in response to intracellular injection of cAMP and cGMP, significantly increasing horizontal cell input

resistance (Miyachi and Murakami, 1991). In a later study, Miyachi et. al. (1994) demonstrated that horizontal cells are decoupled as a result of decreased gap junctional permeability via guanylate cyclase activation due to arachidonic acid application. In contrast, activation of adenylate cyclase due to  $\beta$ -adrenergic receptor stimulation in the turtle cerebrocortex does not affect gap junction permeability (Shin, 1999; personal communication). This indicates that gap junctions may be differentially regulated by cyclic nucleotides in a tissue specific manner.

The neurotransmitter Dopamine has also been shown to modulate the permeability of gap junctions in the turtle brain. Piccolino et. al. (1984) have demonstrated that Dopamine decreases the permeability of the gap junctions between the axon terminals of the H1 horizontal cells of the turtle retina and that this action probably involves cAMP as a second messenger. Dopamine receptor stimulation has also been shown to reduce retinal horizontal cell coupling in other lower vertebrate model systems which include the fish and chick (McMahon and Mattson, 1996; Catsicas et. al., 1998). Although dopamine levels increase significantly in the anoxic turtle brain (Nilsson and Lutz, 1991) its role in regulating neuronal gap junction coupling in the anoxic turtle brain has not yet been investigated.

## SUMMARY AND CONCLUSION

The vertebrate brain is the most oxygen sensitive organ known, suffering irreversible neuronal injury following just minutes of anoxic/ischemic exposure. For example, inhibition of oxygen delivery to the mammalian brain compromises energy dependent  $\text{Na}^+/\text{K}^+$  exchange across the neuronal membrane, facilitating the efflux of  $\text{K}^+$  from the cell. The increase in  $[\text{K}^+]_o$  is thought to cause depolarization of the cell, termed anoxic depolarization, which results in an overwhelming influx of  $\text{Ca}^{2+}$  and  $\text{Na}^+$  into the cell. This increased permeability of the neuron to cations, particularly  $\text{Ca}^{2+}$ , initiates a cascade of intracellular and extracellular excitotoxic events, ultimately causing cell death.

In contrast, the turtle is a notable anoxia tolerant vertebrate in that it has a remarkable ability to withstand prolonged anoxia for several weeks to months depending on temperature. Since 50-60% of the cellular energy budget is dedicated to maintaining cellular ionic gradients via the  $\text{Na}^+/\text{K}^+$  pump, a reduction in turtle membrane ion permeability during anoxia would allow for reduced ATP consumption by the  $\text{Na}^+/\text{K}^+$  pump, thus conserving ATP and increasing survival time. A mechanism which could regulate  $G_w$  is in accordance with the "channel arrest" hypothesis (Hochachka, 1986) which predicts that anoxia tolerant species ought to have mechanisms to acutely regulate cellular ion permeability.

This study has shown that whole cell permeability does decrease in the brain of the western painted turtle during anoxia, supporting the channel arrest hypothesis. The data outline a cellular response to anoxia that includes: increased adenosine levels, stimulation of  $A_1$  receptors, increases in intracellular  $\text{Ca}^{2+}$  and possibly cAMP, activation of protein kinases and phosphatases that target the proposed mechanism capable of changing whole cell permeability and therefore conductance. Furthermore, it is likely that the observed anoxia

induced changes in the cell permeability do not involve changes in neuronal gap junctional coupling in the turtle brain. Thus, it is reasonable to conclude that adenosine and  $\text{Ca}^{2+}$  play a major role in the anoxic regulation of  $G_w$ , and are involved in the natural cellular anoxic defense mechanism of this species.

## References

- Ammermuller, J., Mockel, W., and Perlman, I. (1996) Effects of horizontal cell network architecture on signal spread in the turtle outer retina. Experiments and simulations. *Vision Res.* 36(24):4089-103.
- Ashton, D., Willems, R., Marrannes, R., and Janssen, P.A. (1990) Extracellular ions during veratridine-induced neurotoxicity in hippocampal slices: neuroprotective effects of flunarizine and tetrodotoxin. *Brain Res.* 528(2):212-22.
- Atkinson, D.E. (1977) Cellular energy metabolism and its regulation. New York: Academic Press.
- Ben-Ari, Y. (1990) Galanin and glibenclamide modulate the anoxic release of glutamate in rat CA3 hippocampal neurons. *Eur. J. Neurosci.* 2:62-68.
- Bickler, P.E. (1998) Reduction of NMDA receptor activity in cerebrocortex of turtles (*Chrysemys picta*) during 6wk of anoxia. *Am. J. Physiol.* 275(44):R86-R91.
- Bickler, P.E., and Gallego, S.M. (1993) Inhibition of brain calcium channels by plasma proteins from anoxic turtles. *Am. J. Physiol.* 265(34):R277-R281.
- Bickler, P.E., and Hansen, B.M. (1994) Causes of calcium accumulation in rat cortical brain slices during hypoxia and ischemia: role of ion channels and membrane damage. *Brain Res.* 665(2):269-76.
- Blanton, M., Turco, G., Lo, J.J., and Kriegstein, A.R. (1989) Whole cell recording from neurons in slices of reptilian and mammalian cerebral cortex. *J. Neurosci. Meth.* 30: 203-210.
- Bowersox, S.S., Gadbois, T., Singh, T., Pettus, M., Wang, Y.X., and Luther, R.R. (1996) Selective N-type neuronal voltage-sensitive calcium channel blocker, SNX-111, produces spinal antinociception in rat models of acute, persistent and neuropathic pain. *J. Pharm. Exp. Therap.* 279(3):1243-9.
- Brooks, S.P., and Storey, K.B. (1988) Anoxic brain function: molecular mechanisms of metabolic depression. *FEBS Lett.* 232(1):214-6.
- Buchan, A.M., Gertler, S.Z., Li, H., Xue, D., Huang, Z.G., Chaundy, K.E., Barnes, K., and Lesiuk, H.J. (1994) A selective N-type Ca<sup>2+</sup> channel blocker prevents CA1 injury 24h following severe forebrain ischemia and reduces infarction following focal ischemia. *J. Cereb. Blood Flow Metab.* 14(6):903-10.
- Buck, L.T., and Bickler, P.E. (1995) Role of adenosine in NMDA receptor modulation in the cerebral cortex of an anoxia-tolerant turtle (*Chrysemys picta belli*). *J. Exp. Biol.* 198 ( Pt 7):1621-8.

- Buck, L.T., and Bickler, P.E. (1998) Adenosine and anoxia reduce N-methyl-D-aspartate receptor open probability in turtle cerebrocortex. *J. Exp. Biol.* 201 ( Pt 2):289-97.
- Buck, L.T., Hochachka, P.W., Schon, A., and Gnaiger, E. (1993a) Microcalorimetric measurement of reversible metabolic suppression induced by anoxia in isolated hepatocytes. *Am. J. Physiol.* 265(5 Pt 2):R1014-9.
- Buck, L.T., Land, S.C., and Hochachka, P.W. (1993b) Anoxia-tolerant hepatocytes: model system for study of reversible metabolic suppression. *Am. J. Physiol.* 265(1 Pt 2):R49-56.
- Buckler, K.J. (1997) A novel oxygen-sensitive potassium current in rat carotid body type I cells. *J. Physiol.* 498 (Pt3):649-62.
- Cai, N., and Erdo, S.L. (1992) The effects of Kainate and glutamate agonist, AMPA, are not separable in rat neocortical cultures. *Neurosci. Lett.* 141:57-60.
- Calabresi, P., Pisani, A., and Mercuri, N.B., and Bernardi, G. (1995) On the mechanisms underlying hypoxia induced membrane depolarization in striatal neurons. *Brain* 118(Pt 4): 1027-1038.
- Catsicas, M., Bonness, V., Beckler, D., and Mobbs, P. (1998) Spontaneous Ca<sup>2+</sup> transients and their transmission in the developing chick. *Curr. Biol.* 8(5):283-6.
- Chih, C.P., Feng, Z.C., Rosenthal, M., Lutz, P.L., and Sick, T.J. (1989a) Energy metabolism, ion homeostasis, and evoked potentials in anoxic turtle brain. *Am. J. Physiol.* 257(4 Pt 2):R854-60.
- Chih, C.P., Rosenthal, M., and Sick, T.J. (1989b) Ion leakage is reduced during anoxia in turtle brain: a potential survival strategy. *Am. J. Physiol.* 257(6 Pt 2):R1562-4.
- Choi, D.W. (1990) Cerebral hypoxia: some new approaches and unanswered questions. *J. Neurosci.* 10(8):2493-501.
- Choi, D.W. (1992) Excitotoxic cell death. *J. Neurobiol.* 23:1261-1276.
- Connors, B.W., and Ransom, B.R. (1987) Electrophysiological properties of ependymal cells (radial glia) in dorsal cortex of the turtle *Pseudemys scripta*. *J. Physiol. Lond.* 385: 287-306.
- Dermietzel, R., and Spray, D.C. (1993) Gap junctions in the brain: where, what type, how many and why? *TINS* 16(5):186-192.
- Doll, C.J. (1993a) Anoxic CNS membrane: mechanisms of collapse and stabilization. In: *Surviving Hypoxia: Mechanisms of Control and Adaptation*. Boca Raton: CRC Press, 281-294.

- Doll, C.J., Hochachka, P.W., and Reiner, P.B. (1993b) Reduced ionic conductance in the turtle brain. *Am. J. Physiol.* 265: R929-R933.
- Doll, C.J., Hochachka, P.W., and Hand, S.C. (1994) A microcalorimetric study of turtle cortical slices: insights into brain metabolic depression. *J. Exp. Biol.* 191:141-153.
- Doll, C.J., Hochachka, P.W., and Reiner, P.B. (1991) Channel arrest: implications from membrane resistance in turtle neurons. *Am. J. Physiol.* 261: R1321-R1324.
- Donnelly, D.F., Jiang, C., and Haddad, G.G. (1992) Comparative responses of brain stem and hippocampal neurons to O<sub>2</sub> deprivation: in vitro intracellular studies. *Am J Physiol* 262(5 Pt 1):L549-L554.
- Edwards, A., Lutz, P.L., and Baden, D.G. (1989) Relationship between energy expenditure and ion channel density in the turtle and rat brain. *Am. J. Physiol.* 257(26):R1354-R1358.
- Fay, R.R., and Ream, T.J. (1992) The effects of temperature change and transient hypoxia on auditory nerve fibre response in the goldfish (*Carassius auratus*). *Hearing Res.* 58:9-18.
- Feng, Z.C., Rosenthal, M., and Sick, T.J. (1988) Suppression of evoked potentials with continued ion transport during anoxia in turtle brain. *Am. J. Physiol.* 255(3 Pt 2):R478-84.
- Fink, M., Duprat, F., Lesage, F., Reyes, R., Romey G., Heurteaux, C., and Lazdunski, M. (1996) Cloning, functional expression and brain localization of a novel unconventional outward rectifier K<sup>+</sup> channel. *EMBO J.* 15: 6854-6862.
- Firsov, M.L. and Green, D.G. (1998) Photoreceptor coupling in turtle retina. *Visual Neurosci.* 15(4):755-64.
- Folbegrova, J., Minamisawa, H., Ekholm, A., and Siesjo, B.K. (1990) Phosphorylase a and labile metabolites during anoxia: correlation to membrane fluxes of K<sup>+</sup> and Ca<sup>2+</sup>. *J. Neurochem.* 55:1690-1696.
- Friedman, J.E., and Haddad, G.G. (1994) Anoxia induces an increase in intracellular sodium in rat central neurons in vitro. *Brain Res.* 663(2):329-34.
- Fujiwara, N., Higashi, H., Shimoji K., and Yoshimura, M. (1987). Effects of hypoxia on rat hippocampal neurones in vitro. *J. Physiol.* 384:131-151.
- Gaur, S., Newcomb, R., Rivnay, B., Bell, J.R., Yamashiro, D., Ramachandran, J., and Miljanich, G.P. (1994) Calcium channel antagonist peptides define several components of transmitter release in the hippocampus. *Neuropharmacology* 33(10):1211-9.
- Gleitz, J., Tosch, C., Beile, A., and Peters, T. (1996) The protective action of tetrodotoxin and (+/-)-kavain on anaerobic glycolysis, ATP content and intracellular Na<sup>+</sup> and Ca<sup>2+</sup> of anoxic brain vesicles. *Neuropharmacology* 35(12):1743-52.

- Gulley, R.L., and Reese, T.L. (1981) Cytoskeletal organization at the postsynaptic complex. *J. Cell Biol.* 91:298-302.
- Haddad, G.G., and Jiang, C. (1993) O<sub>2</sub> deprivation in the central nervous system: on mechanisms of neuronal response, differential sensitivity and injury. *Prog. Neurobiol.* 40(3):277-318.
- Hampson, E.C.G.M., Vaney, D.I. and Weiler, R. (1992) Dopaminergic modulation of gap junction permeability between amacrine cells in mammalian retina. *J. Neurosci.* 12: 4911-4922.
- Hampson, E.C.G.M., Weiler, R. and Vaney, D.I. (1994) pH-gated dopaminergic modulation of horizontal cell gap junctions in mammalian retina. *Proc. R. Soc. Lond. B. Biol. Sci.* 255: 67-72.
- Hansen, A.J. (1985) Effect of anoxia on ion distribution in the brain. *Physiol. Rev.* 65:101-148.
- Herbert, C.V., and Jackson, D.C. (1985a) Temperature effects on the responses to prolonged submergence in the turtle *Chrysemys picta bellii*. i. blood acid-base and ionic changes during and following anoxic submergence. *Physiol. Zool* 58: 655-669.
- Herbert, C.V., and Jackson, D.C., (1985b) Temperature effects on the responses to proplonged submergence in the turtle *Chrysemys picta belli* !!. Metabolic rate, blood acid-base and ionic changes, and cardiovascular function in aerated and anoxic water. *Physiol. Zool.* 58: 670-681.
- Hille, B. (1992) Ionic channels of excitable membranes. Saunderland: Sinauer Associates.
- Hochachka, P.W. (1986) Defense strategies against hypoxia and hypothermia. *Science* 231(4735):234-41.
- Hochachka, P. W. (1986) Defense strategies against hypoxia and hypothermia. *Science* 231: 234-241.
- Hochachka, P.W., and Somero G.N. (1984) Biochemical Adaptation. Princeton: Princeton University Press.
- Hochachka, P.W., Lutz, P.L., Sick, T. et. al. ed(s). (1993) Surviving Hypoxia: Mechanisms of Control and Adaptation. Boca Raton: CRC Press, 281-294.
- Hodgkin, A.L., and Huxley, A.F. (1952) Currents carried by sodium and potassium ions through the membrane of the giant axon of *Loligo*. *J. Physiol.* 116:473-496.



- Hylland, P., Nilsson, G.E., and Johansson, D. (1995) Anoxic brain failure in an ectothermic vertebrate: release of amino acids and  $K^+$  in rainbow trout thalamus. *Am. J. Physiol.* 269(5 Pt 2):R1077-84.
- Hylland, P., Nilsson, G.E., and Lutz, P.L. (1994) Time course of anoxia-induced increase in cerebral blood flow rate in turtles: evidence for a role of adenosine. *J. Cereb. Blood Flow Metab.* 14(5):877-81.
- Ikura, M. (1996) Calcium binding and conformational response in EF-hand proteins. *Trends Biochem. Sci.* 21: 14-17.
- Jackson, D.C. (1968) Metabolic depression and oxygen depletion in the diving turtle. *J. Appl. Physiol.* 24(4):503-9.
- Jackson, D.C., and Heisler, N. (1983) Intracellular and extracellular acid-base and electrolyte status of submerged anoxic turtles at 3°C. *Respir. Physiol.* 53(2):187-201.
- Janssen-Bienhold, U., Dermietzel, R., and Weiler, R. (1998) Distribution of connexin43 immunoreactivity in the retinas of different vertebrates. *J. Comp. Neurol.* 396(3):310-21.
- Jeffreys, J.G.R. (1995) Nonsynaptic modulation of neuronal activity in the brain: electric currents and extracellular ions. *Physiol. Rev.* 75:689-723.
- Johansson, D., Nilsson, G., and TÖRnblom, E. (1995) Effects of anoxia on energy metabolism in crucian carp brain slices studied with microcalorimetry. *J. Exp. Biol.* 198(Pt 3):853-9.
- Kaila, K., and Voipio, J. (1987) Postsynaptic fall in intracellular pH induced by GABA-activated bicarbonate conductance. *Nature* 330(6144):163-5.
- Kandler, K., and Katz, L.R. (1995) Neuronal coupling and uncoupling in the developing nervous system. *Curr. Opin. Neurobiol.* 5: 98-105.
- Keller, B.U., Hollmann, M., Heinemann, S., and Konnerth, A. (1992) Calcium influx through subunits GluR1/GluR3 of kainate/AMPA receptor channels is regulated by cAMP dependent protein kinase. *EMBO J.* 11(3):891-6.
- Kelly, D.A., and Storey, K.B. (1988) Organ-specific control of glycolysis in anoxic turtles. *Am. J. Physiol.* 255(5 Pt 2):R774-9.
- Ketchum, K.A., Joiner, W.J., Sellers, A.J., Kaczmarek, L.K., and Goldstein, S.A. (1995) A new family of outwardly rectifying potassium channel proteins with two pore domains in tandem. *Nature* 376:85-88.
- Koh, J.Y., Goldberg, M.P., Hartley, D.M., and Choi, D.W. (1990) Non-NMDA receptor mediated neurotoxicity in cortical culture. *J. Neurosci.* 10:693-705.

- Krnjevic, K., and Leblond J. (1988). Are there hippocampal ATP-sensitive K<sup>+</sup> channels that are activated by anoxia? *Eur. J. Physiol.* 411:R145-R151.
- Land, S.C., and Hochachka, P.W. (1994) Protein turnover during metabolic arrest in turtle hepatocytes: role and energy dependence of proteolysis. *Am. J. Physiol.* 266(4 Pt 1):C1028-36.
- Land, S.C., Buck, L.T., and Hochachka, P.W. (1993) Response of protein synthesis to anoxia and recovery in anoxia-tolerant hepatocytes. *Am. J. Physiol.* 265(1 Pt 2):R41-8.
- Leonoudakis, D., Gray, A.T., Winegar, B.D., Kindler, C.H., Harata, M., Taylor, D.M., Chavez, R.A., Forsayeth, J.R., and Yost, C.S. (1998) An open rectifier potassium channel with two pore domains in tandem cloned from rat cerebellum. *J. Neurosci.* 18(3): 868-877.
- Lesage, F., Guillemare, E., Fink, M., Duprat, F., Lazdunski, M., Romey, G., and Barhanin, J. (1996a) A pH-sensitive yeast outward rectifier K<sup>+</sup> channel with two pore domains and novel gating properties. *J. Biol. Chem.* 271:4183-4187.
- Lesage, F., Guillemare, E., Fink, M., Duprat, F., Lazdunski, M., Romey, G., and Barhanin, J. (1996b) TWIK-1, a ubiquitous human weakly inward rectifying K<sup>+</sup> channel with a novel structure. *EMBO J.* 15:1004-1011.
- Lesage, F., Lauritzen, I., Duprat, F., Reyes, R., Fink, M., Heurteaux, C., and Lazdunski, M. (1997) The structure, function and distribution of the mouse TWIK-1 K<sup>+</sup> channel. *FEBS Lett.* 402: 28-32.
- Lipton, P., and Whittingham, T.S., (1982) Reduced ATP concentrations as a basis for synaptic transmission failure during hypoxia in the in vitro guinea-pig hippocampus. *J. Physiol.* 325:51-56.
- Lutz, P.L. (1992) Mechanisms for anoxic survival in the vertebrate brain. *Annu. Rev. Physiol.* 54:601-18.
- Lutz, P.L., and Leone-Kabler, S.L. (1995) Upregulation of the GABAA/benzodiazepine receptor during anoxia in the freshwater turtle brain. *Am. J. Physiol.* 268(5 Pt 2):R1332-5.
- Lutz, P.L., and Nilsson, G.E. (1994) *The Brain without Oxygen, Causes of failure and mechanisms of survival.* Austin: R. G. Landes.
- Lutz, P.L., and Nilsson, G.E. (1997) *The brain without oxygen.* New York: Landes Bioscience and Chapman & Hall.
- Lutz, P.L., McMahon, P., Rosenthal, M., and Sick, T.J. (1984) Relationships between aerobic and anaerobic energy production in turtle brain in situ. *Am. J. Physiol.* 247(4 Pt 2):R740-4.

- Lutz, P.L., Rosenthal, M., and Sick, T.J., (1985) Living without oxygen: turtle brain as a model of anaerobic metabolism. *Mol. Physiol.* 8:411-425.
- MacVicar, B.A., and Dudek, F.E. (1981) Electrotonic coupling between pyramidal cells: a direct demonstration in rat hippocampal slices. *Science* 213: 782-785.
- McBride, B.W., and Milligan, L.P. (1985) Magnitude of ouabain-sensitive respiration of lamb hepatocytes (*Ovis aries*). *Int. J. Biochem.* 17(1):43-9.
- McGroarty, A., and Greenfield, S.A. (1996) Blockade of dopamine storage, but not of dopamine synthesis, prevents activation of a tolbutamide-sensitive  $K^+$  channel in the guinea-pig substantia nigra. *Exp. Brain. Res.* 110:360-366.
- McMahon, D.G. and Mattson, M.P. (1996) Horizontal cell electrical coupling in the giant danio: synaptic modulation by dopamine and synaptic maintenance by calcium. *Brain Res.* 718:89-96.
- Miyachi, E., and Murakami, M. (1991) Synaptic inputs to turtle horizontal cells analyzed after blocking of gap junctions by intracellular injection of cyclic nucleotides. *Vision Res.* 31(4):631-5.
- Miyachi, E., Kato, C., and Nakaki, C. (1994) Arachidonic acid blocks gap junctions between retinal horizontal cells. *Neuroreport* 5(4):485-8.
- Mourre, C., Ben-Ari, Y., Bernardi H., Fosset, M., and Lazdunski, . (1989) Antidiabetic sulfonylureas: localization of binding sites in the brain and effects on the hyperpolarization induced by anoxia in hippocampal slices. *Brain. Res.* 486:159-164.
- Newby, A.C., Worku, C.Y., Meghi, P., Nakazawa, M., and Skladanowski, A.C. (1990) Adenosine: a retaliatory metabolite or not? *News Physiol. Sci.* 5:67-70.
- Nilsson, G.E. (1990) Long-term anoxia in crucian carp: changes in the levels of amino acid and monoamine neurotransmitters in the brain, catecholamines in chromaffin tissue, and liver glycogen. *Exp. Biol.* 150:295-320.
- Nilsson, G.E. (1992) Evidence for a role of GABA in metabolic depression during anoxia in crucian carp (*Carassius carassius*). *J. Exp. Biol.* 164:243-259.
- Nilsson, G.E. and Lutz, P.L. (1991) Release of inhibitory neurotransmitters in response to anoxia in the turtle brain. *Am. J. Physiol.* 261:R32-R37.
- Nilsson, G.E., Alfaro, A.A., and Lutz, P.L. (1990) Changes in turtle brain neurotransmitters and related substances during anoxia. *Am. J. Physiol.* 259(2 Pt 2):R376-84.

- Nilsson, G.E., and Lutz, P.L. (1991) Release of inhibitory neurotransmitters in response to anoxia in turtle brain. *Am. J. Physiol.* 261(1 Pt 2):R32-7.
- Nilsson, G.E., and Lutz, P.L. (1992) Adenosine release in the anoxic turtle brain as a mechanism for anoxic survival. *J. Exp. Biol.* 162:345-351.
- Nilsson, G.E., Lutz, P.L., and Jackson, T.L. (1991) Neurotransmitters and anoxic survival in the brain: a comparison between anoxia tolerant and anoxia intolerant vertebrates. *Physiol. Zool.* 64:638-652.
- Ozawa, S., Iino, M., and Tsuzuki, K. (1991) Two types of kainate response in cultured rat hippocampal neurons. *J. Neurophysiol.* 66(1):2-11.
- Pek, M., and Lutz, P.L. (1997) Role for adenosine in channel arrest in the anoxic turtle brain. *J. Exp. Biol.* 200 ( Pt 13):1913-7.
- Perez-Pinzon, M.A., Bedford, J., and Rosenthal, M. (1991) Metabolic adaptation to anoxia in the isolated turtle cerebellum. *Soc. Neurosci.* 17:1269 (abst.).
- Perez-Pinzon, M.A., Chan, C.Y., Rosenthal, M., and Sick, T.J. (1992a) Membrane and synaptic activity during anoxia in the isolated turtle cerebellum. *Am. J. Physiol* 263(5 Pt 2):R1057-63.
- Perez-Pinzon, M.A., Rosenthal, M., Lutz, P.L., and Sick, T.J. (1992b) Anoxic survival of the isolated cerebellum of the turtle *Pseudemys scripta elegans*. *Comp. Physiol. [B]* 162(1):68-73.
- Perez-Pinzon, M.A., Rosenthal, M., Sick, T.J., Lutz, P.L., Pablo, J., and Mash, D. (1992c) Downregulation of sodium channels during anoxia: a putative survival strategy of turtle brain. *Am. J. Physiol.* 262(4 Pt 2):R712-5.
- Perez-Pinzon, M.A., Lutz, P.L., Sick, T.J., and Rosenthal, M. (1993) Adenosine, a 'retaliatory' metabolite, promotes anoxia tolerance in the turtle brain. *J. Cereb. Blood Flow Metab.* 13:728-732.
- Piccolino, M., Neyton, J., and Gerschenfeld, H.M. (1984) Decrease of gap junction permeability induced by dopamine and cyclic adenosine 3':5'-monophosphate in horizontal cells of turtle retina. *J. Neurosci.* 4(10):2477-88.
- Pizzi, M., Ribola, M., Valerio, A., Memo, M., and Spano, P. (1991) Various Ca<sup>2+</sup> entry blockers prevent glutamate-induced neurotoxicity. *Eur. J. Pharmacol.* 209(3):169-73.
- Pringle, A.K., Iannotti, F., Wilde, G.J., Chad, J.E., Seeley, P.J., and Sundstrom, L.E. (1997) Neuroprotection by both NMDA and non-NMDA receptor antagonists in in vitro ischemia. *Brain Res.* 755(1):36-46.

- Ridge, J.W. (1972) Hypoxia and the energy charge of the cerebral adenylate pool. *Biochem. J.* 127:351-355.
- Robin, E.D., Lewiston, N., Newman A., Simonm L.M., and Theodore, J. (1979) Bioenergetic pattern of turtle brain and resistance to profound loss of mitochondrial ATP generation. *Proc. Natl. Acad. Sci. U S A* 76(8):3922-6.
- Robin, E.D., Vester, J.W., Murdaugh, H.V., and Millen, J.E. (1964) Prolonged anaerobiosis in a vertebrate: anaerobic metabolism in the freshwater turtle. *J. Cell. Comp. Physiol.* 63:287-297.
- Rosenmund, C., and Westbrook, G.L. (1993) Calcium-Induced Actin depolymerization reduces NMDA channel activity. *Neuron* 10:805-814.
- Rudolphi, K.A., Schubert, P., Parkinson, F.E., and Fredholm, B.B. (1992) Adenosine and brain ischemia. *Cerebrovasc. Brain Metab. Rev.* 4:346-369.
- Sattler, R., Xiong, Z., Lu, W-Y., Hafner, M., MacDonald, J.F., and Tymiansky, M. (1999) Specific coupling of NMDA receptor activation to Nitric Oxide Neurotoxicity by PSD-95 protein. *Science* 284:1845-48.
- Schurr, A., and Rigor, B.M. (1993) Kainate toxicity in energy-compromised rat hippocampal slices: differences between oxygen and glucose deprivation. *Brain Res.* 614(1-2):10-4.
- Seutin V., Shen, K-Z., North, R.A., and Johnson, S.W. (1996) Sulfonylurea-sensitive potassium current evoked by sodium-loading in rat midbrain dopamine neurons. *Neuroscience.* 71(3): 709-719.
- Sheng, M., and Wysznski, M. (1997) Ion channel targeting in neurons. *BioEssays* 19(10):847-853.
- Shiosaka, S., Yamamoto, T., Hertzberg, E.L., and Nagy, J.I. (1989) Gap junction protein in rat hippocampus: correlative light and electron microscope immunohistochemical localization. *J. Comp. Neurol.* 281: 282-291.
- Sick, T.J., Rosenthal, M., LaMana, J.C. and Lutz, P.L. (1982) Brain potassium ion homeostasis, anoxia , and metabolic inhibition in turtle and rats. *Am. J. Physiol.* 243: R281-R288.
- Siesjo, B.K. (1978) *Brain Energy Metabolism.* New York: Wiley.
- Simen, A.A., and Miller, R.J. (1998) Structural features determining differential receptor regulation of neuronal Ca channels. *J. Neurosci.* 18(10):3689-98.

- Suzue, T., Wu, G-B., and Furukawa, T. (1987) High susceptibility to hypoxia of afferent synaptic transmission in the goldfish sacculus. *J. Neurophysiol.* 58:1066-1079.
- Trivedi, B., and Danforth, W.H. (1966) Effect of pH on the kinetics of frog muscle phosphofructokinase. *J. Biol. Chem.* 241(17):4110-2.
- Ultsch, G. (1985) The viability of neararctic freshwater turtles submerged in anoxia and normoxia at 3 and 10°C. *Comp. Biochem. Physiol.* 81A: 607-611.
- Ultsch, G.R., and Jackson, D.C. (1982) Long term submergence at 3°C of the turtle *Chrysemys picta belli* in normoxic and severely hypoxic water. I. Survival, gas exchange and acid-base status. *J. Exp. Biol.* 96:11-28.
- Valentino K, Newcomb R, Gadbois T, Singh T, Bowersox S, Bitner S, Justice A, Yamashiro D, Hoffman BB, Ciaranello R, et al (1993) A selective N-type calcium channel antagonist protects against neuronal loss after global cerebral ischemia. *Proc. Natl. Acad. Sci. U S A* 90(16):7894-7.
- Van der Boon, J., de Jong, R.L., Van den Thillart, G.E., and Addink, A.D. (1992) Reversed-phase ion-paired HPLC of purine nucleotides from skeletal muscle, heart and brain of the goldfish, *Carassius auratus* L.--II. Influence of environmental anoxia on metabolite levels. *Comp. Biochem. Physiol.* [B] 101(4):583-6.
- Van Ginneken, V., Nieveen, M., Van Eersel, R., Van den Thillart, G., and Addink, A. (1996) Neurotransmitter levels and energy status in brain of fish species with and without the survival strategy of metabolic depression. *Comp. Biochem. Physiol.* A. 114:189-196.
- Van Waarde, A., Van den Thillart, G., and Kesbeke, F. (1983) Anaerobic energy metabolism of the European eel, *Anguilla anguilla* L. *J. Comp. Physiol.* 149:469-475.
- Van Waversfeld, J., Addink, A.D.F., and Van den Thillart, G. (1989) Simultaneous direct and indirect calorimetry on normoxic and anoxic goldfish. *J. Exp. Biol.* 142:325-335.
- Westenbroek, R.E., Hell, J.W., Warner, C., Dubel, S.J., Snutch, T.P., and Catterall, W.A. (1992) Biochemical properties and subcellular distribution of an N-type calcium channel alpha 1 subunit. *Neuron* 9(6):1099-115.
- Wheeler, D.B., Randall, A., and Tsien, R.W. (1994) Roles of N-type and Q-type Ca<sup>2+</sup> channels in supporting hippocampal synaptic transmission. *Science* 264(5155):107-11.
- Xia, Y., and Haddad, G.G. (1993) Neuroanatomical distribution and binding properties of saxitoxin sites in the rat and turtle CNS. *J. Comp. Neurol.* 330(3):363-80.
- Xie, H, and Ziskind-Conhaim, L. (1995) Blocking Ca(2+)-dependent synaptic release delays motoneuron differentiation in the rat spinal cord. *J. Neurosci.* 15(9):5900-11.

Xie, Y., Dengler, K., Zacharias, E., Wilffert, B., and Tegtmeier, F. (1994) Effects of the sodium channel blocker tetrodotoxin (TTX) on cellular ion homeostasis in rat brain subjected to complete ischemia. *Brain Res.* 652(2):216-24.

Yu, S.P., Yeh, C.-H., Strasser, U., Tian, M., and Choi, D.W. (1999) NMDA receptor-mediated  $K^+$  efflux and neuronal apoptosis. *Science* 284:336-8.